AD-A092 631 UNIVERSITY COLL LONDON (ENGLAND) DEPT OF PHYSICS AND--ETC F/G 4/1
TROPOSPHERIC - STRATOSPHERIC TIDAL INVESTIGATIONS. HOUGH COMPON--ETC(U)
JUN 80 G V GROVES AFOSR-77-3224

UNCLASSIFIED AFGL-TR-80-0351 NL

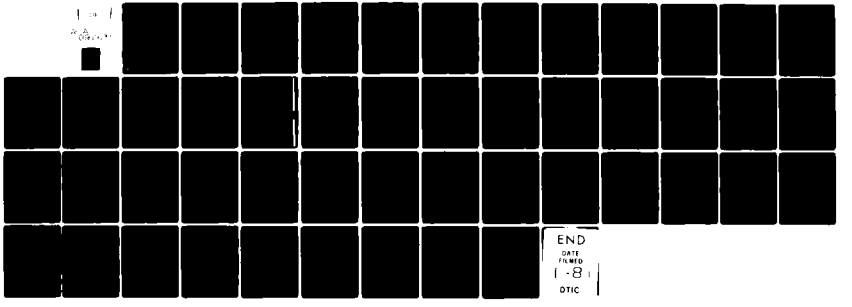

END
DATE FILMED
1-81
DTIC

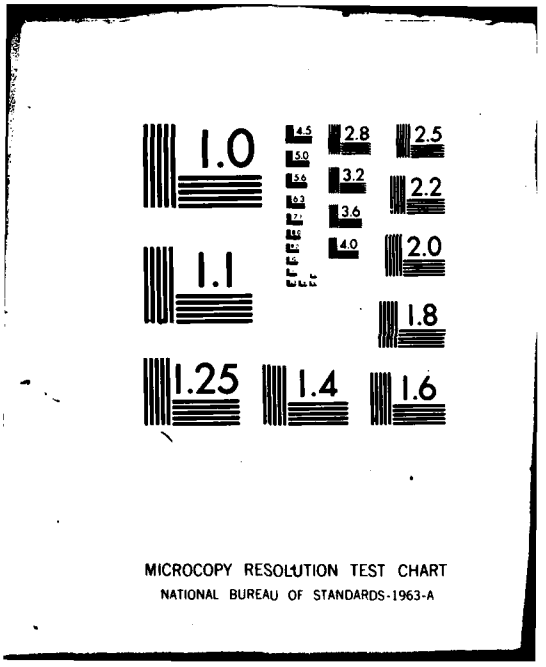
1.0
1.1
1.25
1.4
1.6
1.8
2.0
2.2
2.5
2.8
3.2
3.6
4.0
4.5
5.0
5.6
6.3
7.1
MICROCOPY RESOLUTION TEST CHART
NATIONAL BUREAU OF STANDARDS-1963-A

Grant number: AFOSR – 77 – 3224

# TROPOSPHERIC – STRATOSPHERIC TIDAL INVESTIGATIONS

# HOUGH COMPONENTS OF OZONE HEATING

G. V. Groves
Department of Physics and Astronomy,
University College London,
Gower Street, London WC1E 6BT
England.



30 June 1980

Interim Scientific Report No. 4
1 December 1976 – 30 April 1980



Prepared for:

Air Force Geophysics Laboratory,
L. G. Hanscom Field, Bedford, Massachusetts 01730, USA

European Office of Aerospace Research and Development,
London, England.

| REPORT DOCUMENTATION PAGE | READ INSTRUCTIONS BEFORE COMPLETING FORM |
|---|---|
| 1. Report Number AFGL-TR-80-0351 | 2. Govt Accession No. AD-A092 632 | 3. Recipient's Catalog Number |
| 4. Title (and Subtitle) TROPOSPHERIC - STRATOSPHERIC TIDAL INVESTIGATIONS: Hough components of ozone heating. | 5. Type of Report & Period Covered Scientific Report No. 4. 1 December 1976 - 30 April 1980. |
| | 6. Performing Org. Report Number |
| 7. Author(s) G. V. Groves | 8. Contract or Grant Number AFOSR - 77 - 3224 |
| 9. Performing Organization Name and Address Department of Physics and Astronomy, University College London, Gower Street, London WC1E 6BT, England. | 10. Program Element, Project, Task Area & Work Unit Numbers 62101F 668705AJ |
| 11. Controlling Office Name and Address Air Force Geophysics Laboratory, Hanscom AFB, Massachusetts 01731 Monitor/William K. Vickery/LKD | 12. Report Date 30 June 1980 |
| | 13. Number of Pages 47 |
| 14. Monitoring Agency Name and Address European Office of Aerospace Research and Development, Box 14, FPO, New York 09510, USA. | 15. Unclassified |
| 16. & 17. Distribution Statement Approved for public release; distribution unlimited. | |
| 18. Supplementary Notes | |
| 19. Key Words Atmosphere, ozone, heating, tides | |

20. Abstract

Formulae are derived for the Hough components and the mean rate of solar radiational heating by ozone absorption in the presence of a lower reflecting layer. A model of ozone densities based on observational data is presented for each of the four seasonal months January, April, July and October at heights 0(5)80 km and latitudes 0(15)90°. Diurnal and semi-diurnal components of heating are evaluated for migrating modes and discussed in relation to features of the adopted ozone model. Comparisons are made with earlier evaluations.

FORM 1473

# Hough components of ozone heating

G. V. Groves
Department of Physics and Astronomy,
University College London,
England

## Abstract

Formulae are derived for the Hough components and the mean rate of solar radiational heating by ozone absorption in the presence of a lower reflecting layer. A model of ozone densities based on observational data is presented for each of the four seasonal months January, April, July and October at heights 0(5)80 km and latitudes 0(15)90°. Diurnal and semi-diurnal components of heating are evaluated for migrating modes and discussed in relation to features of the adopted ozone model. Comparisons are made with earlier evaluations.

CONTENTS

## 1. Introduction

A major source of thermal excitation of atmospheric tides is that of absorption of solar radiation by ozone. Calculations by Butler and Small (1963) showed that heating in the region of 50 km altitude contributes significantly to surface pressure oscillations through particular modes of oscillation, notably the leading semi-diurnal (2,2,2) mode. From ozone absorption cross-sections, solar spectral data and height profiles of ozone concentration, heating rates may be calculated for a given time of the year at given heights, latitudes and times of day. By extracting the appropriate Fourier time component (e.g. diurnal or semi-diurnal) and taking the latitudinal average weighted by the selected Hough function, the corresponding component of the heating rate is obtained. Lindzen (1967) obtained diurnal Hough components of equinox heating from the radiative-photochemical model of Leovy (1964). Semi-diurnal components have likewise been derived (Chapman and Lindzen, 1970; Lindzen and Hong, 1974; Hong and Lindzen, 1976).

The purpose of this paper is to evaluate the (1,1,1), (2,2,2) and other diurnal and semi-diurnal Hough components of ozone heating in each of the four seasons of the year on the basis of observed ozone concentrations. Particular attention is given to the construction of a seasonal-latitudinal ozone model (§4). For calculating the solar

energy absorption at many heights with global coverage a rapid method of computation is required. To meet this need the parametric treatment of Lacis and Hansen (1974) has been adopted and is described in §2.

## 2. Formulation of heating rate due to ozone absorption

Let $A$ be the ozone absorption at height z of solar radiation incident on the atmosphere at zenith distance $\zeta$, then the rate of heating within a cylindrical volume of unit horizontal base area and height dz inclined at an angle $\zeta$ to the vertical is $-S_o \cos\zeta \, dA$, where $S_o$ is solar energy flux and dA is the increase in A corresponding to an increase dz in z. The heating rate per unit mass of atmosphere is then

$$J_a = -\frac{\nu S_o}{\rho}\frac{dA}{dz} \qquad (2.1)$$

where $\rho$ is air density and

$$\nu = \cos\zeta \qquad (2.2)$$

$S_o$ is taken as 0.1353 W $cm^{-2}$ (Thekaekara, 1973) with an inverse square dependence on the Sun-Earth distance. By spherical trigonometry

$$\nu = \cos\theta \sin\delta + \sin\phi \cos\delta \cos t' \qquad (2.3)$$

where $\delta$ is solar declination, $\theta$ is colatitude and $\pi + t'$ is local time in radians.

To evaluate the derivative in (2.1) we use the parameterization for ozone absorption of Lacis and Hansen (1974)

$$A_o = \frac{0.02119\,x}{1 + 0.042x + 0.000323x^2} + \frac{1.082x}{(1+138.6x)^{0.805}} + \frac{0.0658x}{1+(103.6x)^3} \qquad (2.4)$$

where

$$x = uM \qquad (2.5)$$

u is the ozone amount (in cm at NTP) in a vertical column above height z and M is the magnification factor due to slant path and refraction

$$M = 35/(1224\nu^2 + 1)^{\frac{1}{2}} \qquad (2.6)$$

The first term on the right-hand side of (2.4) relates to absorption at visual wavelengths and has a numerical precision of nearly four decimals in the interval $10^{-4} \leqslant x \leqslant 10$ cm. The second and third terms relate to ultraviolet absorption and are accurate to within 0.5 per cent in the interval $10^{-4} \leqslant x \leqslant 1$ cm.

In (2.1) dA/dz would be equal to $dA_o/dz$ in the absence of a reflecting layer beneath the ozone absorbing region. In general reflections from the surface and lower atmosphere

provide an upward flux of diffuse radiation and

$$\frac{dA}{dz} = \frac{dA_o(x)}{dz} - R\,\frac{dA_o(x')}{dz} \qquad (2.7)$$

where x' is the ozone path length traversed by solar radiation on reaching height z from below. We have

$$x' = u_t M + (u_t - u)\bar{M} \qquad (2.8)$$

where $u_t$ is the total ozone amount in a vertical path above the reflecting layer (the surface for clear sky conditions or the cloud tops for cloudy skies) and $\bar{M} = 1.9$ is an effective magnification factor for the upward diffuse radiation. The negative sign arises in (2.7) as $A_o(x')$ decreases with z whereas A(x) increases with z. R is the albedo of the reflecting layer and depends on the effective albedo of the lower atmosphere $R_a$ and the surface albedo $R_g$. It may be shown that (Lacis and Hansen, 1974)

$$R = R_a + (1 - R_a)(1 - \bar{R}_a) R_g / (1 - \bar{R}_a R_g) \qquad (2.9)$$

$R_a$ and hence R are functions of $\nu$, and $\bar{R}_a$ is defined by

$$\bar{R}_a = 2\int_0^1 R_a(\nu)\,\nu\,d\nu \qquad (2.10)$$

Let (1-K) be the fraction of cloud-free sky having an albedo (from above) of $R = R_1$ and let $R = R_2$ for the

fraction $\kappa$ of cloudy sky on the assumption that all areas of cloud have the same reflective properties. The albedo of the reflecting layer on neglecting cloud edge effects is

$$R = (1-\kappa) R_1 + \kappa R_2 \qquad (2.11)$$

On adopting the relations of Lacis and Hansen (1974) for the reflectivity of a cloud-free atmosphere $R_{a1}$ and of a cloudy atmosphere $R_{a2}$, we obtain $R_1$, $R_2$ from (2.9). We have

$$R_{a1} = 0.219/(1 + 0.816\nu) \qquad (2.12)$$

$$R_{a2} = 0.13\tau/(1 + 0.13\tau) \qquad (2.13)$$

where $\tau$ is the total visual optical thickness of the cloud layer. By (2.10)

$$\bar{R}_{a1} = 0.144 \qquad (2.14)$$

$$\bar{R}_{a2} = 0.13\tau/(1 + 0.13\tau) \qquad (2.15)$$

Hence (2.11) may be written by (2.9), (2.12) to (2.15)

$$R = c_1/(1+0.816\nu) + c_2 \qquad (2.16)$$

where

$$c_1 = 0.219(1-\kappa)(1-b_1) \qquad (2.17)$$

$$c_2 = (1-\kappa) b_1 + \kappa\left[b_2 + (1-b_2) R_{a2}\right] \qquad (2.18)$$

$$b_j = (1-\bar{R}_{aj}) R_g/(1-\bar{R}_{aj} R_g) \qquad (j = 1,2) \qquad (2.19)$$

3. Relations for heating rate components

We express time (G.M.T.) t and longitude $\phi$ in radians and expand $J_a$ as a Fourier series in t in the interval $(0, 2\pi)$

$$J_a = \sum_{m=0}^{\infty} \left( J_m^R \cos mt + J_m^I \sin mt \right) \qquad (3.1)$$

$m = 1,2,..$ relate to the diurnal, semi-diurnal,.. components of heating. Defining

$$J_m = J_m^R + i\, J_m^I \qquad (3.2)$$

(3.1) may be written as

$$J_a = R\mathrm{l} \sum_{m=0}^{\infty} J_m^* e^{imt} \qquad (3.3)$$

Since $J_m$ is periodic in $\phi$ in the interval $(0, 2\pi)$ it may be expanded as

$$J_m = \sum_{s=0}^{\infty} \left( J_C^s \cos s\phi + J_S^s \sin s\phi \right) \qquad (3.4)$$

where $J_C^s$, $J_S^s$ are complex. It is convenient to replace $J_C^s$, $J_S^s$ by $J_m^{\pm s}$ defined by

$$\begin{aligned} J_m^0 &= J_C^0 \\ 2J_m^s &= J_C^s + i\, J_S^s \qquad (s>0) \\ 2J_m^{-s} &= J_C^s - i\, J_S^s \qquad (s>0) \end{aligned} \qquad (3.5)$$

Then (3.4) becomes

$$J_m = \sum_{s=-\infty}^{\infty} J_m^s e^{-is\phi} \qquad (3.6)$$

and (3.3) becomes

$$J_a = R\Big| \sum_{m,s} J_m^{s*} \, e^{i(mt+s\phi)} \tag{3.7}$$

$J_m^s$ is a function of colatitude $\theta$ which is expanded for $m \neq 0$ in terms of normalized Hough functions $\Theta_{m,n}^s(\mu)$

$$J_m^s = \sum_n J_{m,n}^s \, \Theta_{m,n}^s(\mu) \qquad (m \neq 0) \tag{3.8}$$

where

$$\mu = \cos\theta \tag{3.9}$$

The summation in (3.8) is taken over all members of the set of eigenfunctions of Laplace's tidal equation for given $m\ (\neq 0)$ and s. The full expansion of $J_a$ is then

$$J_a = R\Big| \Big[ \sum_s J_0^{s*}(\mu) e^{is\phi} + \sum_{m\neq 0} \sum_{s,n} J_{m,n}^{s*} \, \Theta_{m,n}^s(\mu) \, e^{i(mt+s\phi)} \Big] \tag{3.10}$$

It may be shown using (3. ~ that

$$\begin{aligned} J_0^0(\mu) &= \frac{1}{4\pi^2} \int_0^{2\pi}\int_0^{2\pi} J_a(\mu,\phi,t)\, dt\, d\phi \\ J_0^s(\mu) &= \frac{1}{2\pi^2} \int_0^{2\pi}\int_0^{2\pi} J_a(\mu,\phi,t)\, e^{is\phi}\, dt\, d\phi \qquad (s \neq 0) \end{aligned} \tag{3.11}$$

and on using the orthogonality properties of $\Theta_{m,n}^s$ that

for $m \neq 0$

$$J^{s}_{m,n} = \frac{1}{2\pi^2}\int_{-1}^{1}\int_{0}^{2\pi}\int_{0}^{2\pi} J_a(\mu,\phi,t)\,\Theta^{s}_{m,n}(\mu)\,e^{i(mt+s\phi)}\,dt\,d\phi\,d\mu \quad (3.12)$$

Local time in radians is expressed by either side of the equation

$$\phi + t = \pi + t' \quad (3.13)$$

Hence from (2.1), (2.7), (2.16), (3.11) and (3.12)

$$\begin{aligned} J^{s}_{o}(\mu) &= \frac{S_o}{4\pi}\int_{0}^{2\pi} F_o\,d\phi \qquad (s=0) \\ &= \frac{S_o}{2\pi}\int_{0}^{2\pi} F_o\,e^{is\phi}\,d\phi \qquad (s\neq 0) \end{aligned} \quad (3.14)$$

$$J^{s}_{m,n} = \frac{S_o}{2\pi}\int_{-1}^{1}\int_{0}^{2\pi} F_m\,\Theta^{s}_{m,n}\,e^{i(s-m)\phi}\,d\phi\,d\mu \quad (m\neq 0) \quad (3.15)$$

where

$$(-)^m F_m = (f_0 + c_1 f_1 + c_2 f_2)/\pi\rho \quad (3.16)$$

$$f_0(z,\mu,\phi) = -\int_{-t_o}^{t_o}\frac{dA_o(z)}{dz}\,\nu\,e^{imt'}\,dt' \quad (3.17)$$

$$f_1(z,\mu,\phi) = \int_{-t_o}^{t}\frac{dA_o(x')}{dz}\,\nu\,(1+0.816\nu)^{-1}\,e^{imt'}\,dt' \quad (3.18)$$

$$f_2(z,\mu,\phi) = \int_{-t_o}^{t_o}\frac{dA_o(x')}{dz}\,\nu\,e^{imt'}\,dt' \quad (3.19)$$

and $-t_o$, $t_o$ are the values of t' at sunrise and sunset

respectively. If no daily variation in ozone concentration is present, u in (2.5) is independent of t' and $e^{imt'}$ may be replaced by $\cos mt'$ as x, x' and $\nu$ are even functions of t'.

If ozone and air density are independent of longitude, (3.14) and (3.15) may be written as

$$\begin{aligned} J_0^s(\mu) &= \tfrac{1}{2} S_0 G_0^0 \qquad (s=0) \\ &= S_0 G_0^s \qquad (s\neq 0) \end{aligned} \tag{3.20}$$

$$J_{m,n}^s = S_0 \int_{-1}^{1} G_m^s \, \Theta_{m,n}^s \, d\mu \qquad (m\neq 0) \tag{3.21}$$

where

$$G_m^s = (C_0 f_0 + C_1 f_1 + C_2 f_2)/\pi\rho \tag{3.22}$$

$$\begin{aligned} C_0 &= 1 \qquad (s=m) \\ &= 0 \qquad (s\neq m) \end{aligned} \tag{3.23}$$

$$C_j = \frac{1}{2\pi}\int_0^{2\pi} c_j \, e^{i(s-m)\phi} \, d\phi \qquad (j=1,2)$$

4. A latitudinal and seasonal ozone model

Table 1 presents a model of ozone concentrations that has been prepared from observational data. At high latitudes and at heights above 50 km observational support is limited and values are of a provisional nature. Below 50 km, data

| | January N | | | | | | | July N | | | | | |
|---|---|---|---|---|---|---|---|---|---|---|---|---|---|
| H | 90 | 75 | 60 | 45 | 30 | 15 | 0 | 15 | 30 | 45 | 60 | 75 | 90 | H |
| km | | | | | | | | | | | | | | |
| 0 | 11.77 | 11.90 | 11.93 | 11.73 | 11.54 | 11.40 | 11.40 | 11.40 | 11.54 | 11.73 | 11.93 | 11.76 | 11.51 | 0 |
| 5 | 11.79 | 11.91 | 12.04 | 11.82 | 11.65 | 11.58 | 11.56 | 11.58 | 11.65 | 11.82 | 12.04 | 11.88 | 11.66 | 5 |
| 10 | 12.27 | 12.45 | 12.47 | 12.38 | 12.13 | 11.79 | 11.65 | 11.66 | 11.89 | 12.26 | 12.30 | 12.19 | 12.01 | 10 |
| 15 | 12.88 | 12.83 | 12.63 | 12.42 | 12.10 | 11.60 | 11.43 | 11.48 | 11.87 | 12.26 | 12.52 | 12.59 | 12.63 | 15 |
| 20 | 12.85 | 12.81 | 12.72 | 12.55 | 12.40 | 12.24 | 12.16 | 12.29 | 12.44 | 12.56 | 12.64 | 12.71 | 12.74 | 20 |
| 25 | 12.55 | 12.56 | 12.60 | 12.66 | 12.62 | 12.60 | 12.64 | 12.66 | 12.66 | 12.63 | 12.56 | 12.50 | 12.48 | 25 |
| 30 | 12.20 | 12.26 | 12.34 | 12.42 | 12.48 | 12.54 | 12.58 | 12.58 | 12.52 | 12.45 | 12.36 | 12.27 | 12.22 | 30 |
| 35 | 11.99 | 12.03 | 12.08 | 12.14 | 12.18 | 12.20 | 12.22 | 12.23 | 12.21 | 12.16 | 12.09 | 12.01 | 11.94 | 35 |
| 40 | 11.79 | 11.80 | 11.80 | 11.79 | 11.76 | 11.72 | 11.73 | 11.75 | 11.76 | 11.73 | 11.70 | 11.70 | 11.72 | 40 |
| 45 | 11.47 | 11.46 | 11.44 | 11.37 | 11.28 | 11.22 | 11.19 | 11.21 | 11.22 | 11.21 | 11.18 | 11.18 | 11.24 | 45 |
| 50 | 11.02 | 11.02 | 10.97 | 10.90 | 10.82 | 10.75 | 10.70 | 10.69 | 10.71 | 10.72 | 10.71 | 10.74 | 10.78 | 50 |
| 55 | 10.47 | 10.47 | 10.47 | 10.45 | 10.39 | 10.34 | 10.28 | 10.24 | 10.23 | 10.23 | 10.24 | 10.27 | 10.29 | 55 |
| 60 | 10.00 | 10.02 | 10.03 | 10.02 | 9.98 | 9.93 | 9.87 | 9.82 | 9.76 | 9.70 | 9.62 | 9.57 | 9.57 | 60 |
| 65 | 9.59 | 9.58 | 9.56 | 9.53 | 9.48 | 9.43 | 9.36 | 9.29 | 9.20 | 9.07 | 8.91 | 8.71 | 8.50 | 65 |
| 70 | 9.08 | 9.01 | 8.95 | 8.89 | 8.84 | 8.78 | 8.72 | 8.64 | 8.54 | 8.40 | 8.23 | 8.01 | 7.77 | 70 |
| 75 | 8.33 | 8.29 | 8.26 | 8.22 | 8.18 | 8.13 | 8.08 | 8.02 | 7.95 | 7.88 | 7.78 | 7.66 | 7.51 | 75 |
| 80 | 7.79 | 7.79 | 7.79 | 7.79 | 7.79 | 7.79 | 7.79 | 7.79 | 7.79 | 7.79 | 7.79 | 7.79 | 7.79 | 80 |

Table 1. Latitudinal cross-sections of log(ozone concentration, $cm^{-3}$) for January N (or July S) and July N (or January S)

| H km | | A - April N / O - October S 90 | 75 | 60 | 45 | 30 | 15 | 0 | October N 15 | 30 | 45 | 60 | 75 | 90 | H |
|---|---|---|---|---|---|---|---|---|---|---|---|---|---|---|---|
| 0 | A | 11.73 | 11.85 | 11.90 | 11.82 | 11.60 | 11.40 | 11.48 | 11.54 | 11.60 | 11.63 | 11.65 | 11.64 | 11.58 | 0 |
| | O | 11.39 | 11.73 | | | | | | | | | | | | |
| 5 | A | 11.78 | 12.04 | 12.09 | 12.06 | 11.65 | 11.60 | 11.57 | 11.63 | 11.70 | 11.74 | 11.76 | 11.74 | 11.69 | 5 |
| | O | 11.47 | 11.86 | | | | | | | | | | | | |
| 10 | A | 12.03 | 12.48 | 12.52 | 12.44 | 12.03 | 11.89 | 11.86 | 11.90 | 12.00 | 12.15 | 12.17 | 12.15 | 12.20 | 10 |
| | O | 11.77 | 12.33 | 12.49 | | | | | | | | | | | |
| 15 | A | 12.79 | 12.73 | 12.63 | 12.50 | 12.18 | 11.81 | 11.74 | 11.60 | 11.93 | 12.25 | 12.41 | 12.51 | 12.56 | 15 |
| | O | 12.55 | 12.59 | 12.60 | | | | | | | | | | | |
| 20 | A | 12.81 | 12.78 | 12.73 | 12.65 | 12.52 | 12.38 | 12.36 | 12.36 | 12.38 | 12.51 | 12.61 | 12.62 | 12.57 | 20 |
| | O | 12.64 | 12.69 | 12.70 | | | | | | | | | | | |
| 25 | A | 12.58 | 12.59 | 12.62 | 12.66 | 12.65 | 12.64 | 12.63 | 12.63 | 12.64 | 12.60 | 12.54 | 12.46 | 12.44 | 25 |
| | O | 12.48 | 12.53 | 12.60 | | | | | | | | | | | |
| 30 | | 12.28 | 12.32 | 12.42 | 12.47 | 12.49 | 12.50 | 12.51 | 12.48 | 12.51 | 12.46 | 12.35 | 12.19 | 12.09 | 30 |
| 35 | | 11.96 | 12.05 | 12.14 | 12.20 | 12.22 | 12.18 | 12.15 | 12.15 | 12.20 | 12.20 | 12.08 | 11.91 | 11.85 | 35 |
| 40 | | 11.65 | 11.72 | 11.76 | 11.80 | 11.80 | 11.71 | 11.66 | 11.69 | 11.76 | 11.82 | 11.81 | 11.71 | 11.60 | 40 |
| 45 | | 11.23 | 11.27 | 11.30 | 11.31 | 11.28 | 11.19 | 11.16 | 11.18 | 11.25 | 11.35 | 11.42 | 11.41 | 11.33 | 45 |
| 50 | | 10.75 | 10.79 | 10.82 | 10.80 | 10.78 | 10.74 | 10.73 | 10.74 | 10.77 | 10.81 | 10.87 | 10.91 | 10.92 | 50 |
| 55 | | 10.27 | 10.31 | 10.33 | 10.33 | 10.33 | 10.33 | 10.33 | 10.33 | 10.30 | 10.26 | 10.26 | 10.20 | 10.11 | 55 |
| 60 | | 9.67 | 9.76 | 9.84 | 9.90 | 9.95 | 9.98 | 9.98 | 9.95 | 9.87 | 9.75 | 9.56 | 9.27 | 8.90 | 60 |
| 65 | | 9.00 | 9.17 | 9.34 | 9.45 | 9.51 | 9.55 | 9.56 | 9.51 | 9.41 | 9.27 | 8.96 | 8.56 | 8.40 | 65 |
| 70 | | 8.57 | 8.68 | 8.77 | 8.83 | 8.88 | 8.90 | 8.90 | 8.86 | 8.80 | 8.70 | 8.46 | 8.22 | 8.22 | 70 |
| 75 | | 8.26 | 8.23 | 8.20 | 8.18 | 8.18 | 8.16 | 8.15 | 8.13 | 8.11 | 8.10 | 8.08 | 8.06 | 8.03 | 75 |
| 80 | | 8.08 | 8.06 | 8.04 | 8.02 | 8.00 | 8.00 | 7.98 | 7.95 | 7.93 | 7.91 | 7.90 | 7.90 | 7.89 | 80 |

Table 1. (continued) April N (or October S) and October N (or April S)

were sufficiently abundant for only those dates falling within the months of January, April, July and October to be used, but at greater heights data for dates up to one month on either side of these months were included.

A longitudinal ozone dependence has been apparent for some time from N hemisphere total ozone amounts (London, 1963). The main feature of the distribution is the existence of three high-latitude regions of maximum ozone over N.E. America, E. Asia and N. Europe which become particularly well developed and steady in late winter and early spring (Khrugian, 1973). Over the last 10 years, satellite techniques have contributed increasingly to ozone measurement (Krueger et al., 1980). Global distributions of total ozone (Prabhakara et al., 1976; Hilsenrath et al., 1979) show good agreement with ground-based measurements and have improved geographical coverage particularly in the S hemisphere. Evidence of longitudinal variations in stratospheric ozone has also been provided by satellite observations (Krueger et al., 1973; Frederick et al., 1977); and a maximum variation at 35 km of about 12 per cent has been observed by the OGO-4 satellite (London et al., 1977). Such data are however inadequate for extending the present model in longitude.

The extended network of ground stations operating

since the I.G.Y. has shown considerable seasonal asymmetries in total ozone amounts between the two hemispheres (Duetsch, 1974). Satellite measurements have generally confirmed these results with improvements in time resolution and S hemisphere coverage (Ghazi et al., 1976; Hilsenrath et al., 1979). For vertical ozone distributions however insufficient data are available for a comparable analysis of seasonal asymmetries. The respective summer, autumn and winter distributions have therefore been represented by the same model for either hemisphere: for spring, the model takes account of the higher values at high N latitudes than at corresponding S latitudes with entries designated A (April N) and O (October S) in Table 1.

The model between 60 N and 60 S is that prepared by Lucas (1978) apart from minor modifications at 60° latitudes and the addition of heights 0, 5 and 80 km. Up to 45 km, the model is based primarily on Umkehr measurements and compares well with earlier analyses. At 35 and 40 km the model depends equally on satellite data and Umkehr observations. Above 55 km, data are extremely sparse and the latitudinal dependence was obtained by fitting a lowest order polynomial, which was often a straight line. A more detailed account of the sources of data and the preparation of the model for latitudes 60 N to 60 S has already been given (Lucas, 1978).

For extending the model to 90° latitude, the following sources have provided data: Ramanathan and Kulkarni (1960); Krueger et al., (1973); Duetsch (1974); London et al., (1977); and Wilcox et al., (1977). Between 60 and 80 km the entries in Table 1 are a simple extrapolation of the values at lower latitudes followed by smoothing in height. Below 50 km just over half the entries in Table 1 are without observational support during the season to which they apply.

Values from Table 1 at 45° latitude are compared in Table 2 with those of the mid-latitude annual mean model that has been adopted for the 1976 U.S. Standard Atmosphere (Krueger and Minzner, 1976). On averaging the January, April, July and October values of the present model at 45° latitude a profile is obtained which agrees with the standard to within 2 per cent at 40 to 70 km. In view of the appreciable seasonal variation at the greater heights, such agreement is remarkably good. Between 15 and 25 km the standard values exceed the average of the seasonal values by amounts of up to 30 per cent (reached at 20 km). At lower heights the average exceeds the standard having a sharp increase in ozone concentration from 4 to 8 km, whereas a similar increase occurs in the standard values between 8 and 12 km: consequently values differ considerably at 10 km (Table 2). Such differences are however largely

Table 2. Comparison between Table 1 values of ozone concentration ($cm^{-3}$) and those of the 1976 U.S. Standard Atmosphere (Krueger and Minzner, 1976)

| Ht km | Jan | Apr | Jul | Oct | Average of 4 seasons | U.S. Standard Atmosphere 1976 | |
|---|---|---|---|---|---|---|---|
| | at 45 N latitude | | | | | | |
| 10 | 24.0 | 27.5 | 18.0 | 14.0 | 20.9 | 11.3 | x $10^{11}$ |
| 20 | 35.5 | 45.0 | 36.5 | 32.5 | 37.4 | 47.7 | x $10^{11}$ |
| 30 | 26.5 | 29.5 | 28.0 | 28.5 | 28.1 | 25.2 | x $10^{11}$ |
| 40 | 61.7 | 63.7 | 54.2 | 66.1 | 61.4 | 60.7 | x $10^{10}$ |
| 50 | 80.2 | 63.7 | 52.0 | 65.0 | 65.2 | 66.4 | x $10^{9}$ |
| 60 | 103.5 | 79.4 | 50.4 | 56.8 | 72.5 | 73.3 | x $10^{8}$ |
| 70 | 78.3 | 68.1 | 25.3 | 49.5 | 55.3 | 54 | x $10^{7}$ |
| Total ozone | 9.48<br>0.353 | 10.89<br>0.405 | 8.60<br>0.320 | 8.24<br>0.307 | 9.30<br>0.346 | 9.27 x $10^{18}$ $cm^{-2}$<br>0.345 atm-cm | |

self-balancing in a vertical integration of the ozone concentration as total ozone amounts agree very closely (Table 2).

Variations of ozone concentration with time of day are shown by the photochemical analysis of Park and London (1974) to be insignificant below 50 km, while above 50 km they increase with height and would appear likely to effect the present calculations at 60-65 km and above. A procedure has therefore been adopted whereby the ozone concentrations of Table 1 at 50 to 80 km are multiplied by a height-dependent factor representing the relative ozone variation between sunrise and sunset. The factor has been based on the calculations of Park and London (1974) for July 30 N and is applied to other seasons and latitudes with rough approximation by expressing its time-dependence as a fraction of the sunrise-sunset interval instead of local time. The observationally derived values of Table 1, being based on techniques limited to daylight conditions, are taken to correspond to the daytime maximum of ozone concentration shown by the theoretical results, i.e. the factor is normalized at each height to a maximum value of unity (Lucas, 1978).

A seasonal-latitudinal model for air density $\rho$, which appears in (3.16) and (3.22), has been employed by taking values from CIRA (1972) between 25 and 80 km altitude and from the U.S. Standard Atmosphere Supplements, 1966 (COESA, 1967) at lower heights.

5. Surface and lower atmosphere reflectivities

A simple representation has been devised for surface albedo $R_g$ by assigning one of the values 0.07, 0.14, 0.21 or 0.75 to each $10^o$ latitude x $10^o$ longitude area according to whether the area is categorized as all sea, half sea and half land, all land or snow covered. No account is taken of daily or seasonal variations of albedo. The albedo of a water surface depends strongly on solar zenith angle and the value 0.07 is that adopted by Katayama (1966) for diffuse solar radiation: the same value was taken by Lacis and Hansen (1974). Values of 0.05 and 0.15 for the average albedos of sea and land surfaces respectively have been assumed by Yamamoto et al., (1974); and surface albedos of 0.1 and 0.4 have been taken to be representative of ocean surface and bright sand (or old dirty snow) by Liou et al., (1978). Land albedos depend on the nature of the surface and vary seasonally when vegetated or subject to snow. A land albedo of 0.21 has been adopted here as this value is an average of the values given by Katayama (1966) for different types of land surface. The value of 0.75 for snow-covered areas is the mean surface albedo calculated by Katayama (1967) for 60 N in January.

For simplicity (2.11) was formulated on the assumption that all cloudy areas have the same reflective properties.

**Katayama** (1967) has calculated an average albedo for cloudy areas of 0.60 (0.62 for January and 0.58 for July) which corresponds to the quantity $R_{a2}$ above being the sum of cloud albedo and a small contribution due to atmospheric scattering above the cloud layer (amounting to about 0.045). By (2.15), the corresponding value of optical thickness is 11.5.

For cloud cover, the four seasonal maps of average daytime cloudiness prepared by Clapp (1964) from Tiros IV, V and VI nephanalyses were adopted. The maps cover 60 N to 60 S and all longitudes, cloud amounts being shown as either $< 0.50$, 0.50-0.75 or $> 0.75$. To each $10^{\circ}$ latitude x $10^{\circ}$ longitude area one of the three cloudiness values 0.25, 0.625 or 0.875 was allocated on the basis of these maps. At 70-$90^{\circ}$ latitudes values were assigned on the basis of the maps of Shaw (1942).

## 6. Ozone heating rates

### 6.1 Mean heating

As a preliminary calculation, mean heating rates at $0^{\circ}$ latitude have been determined for the April ozone profile and different solar zenith angles. Results are plotted in Fig. 1 of $J_a/c_p$ in units of $^{\circ}$/day where $c_p$ is the specific heat of air at constant pressure and $J_a$ is obtained from (2.1). Results are shown for two types of lower reflecting layer:

(i) clear sky, reflexion arising jointly from atmospheric

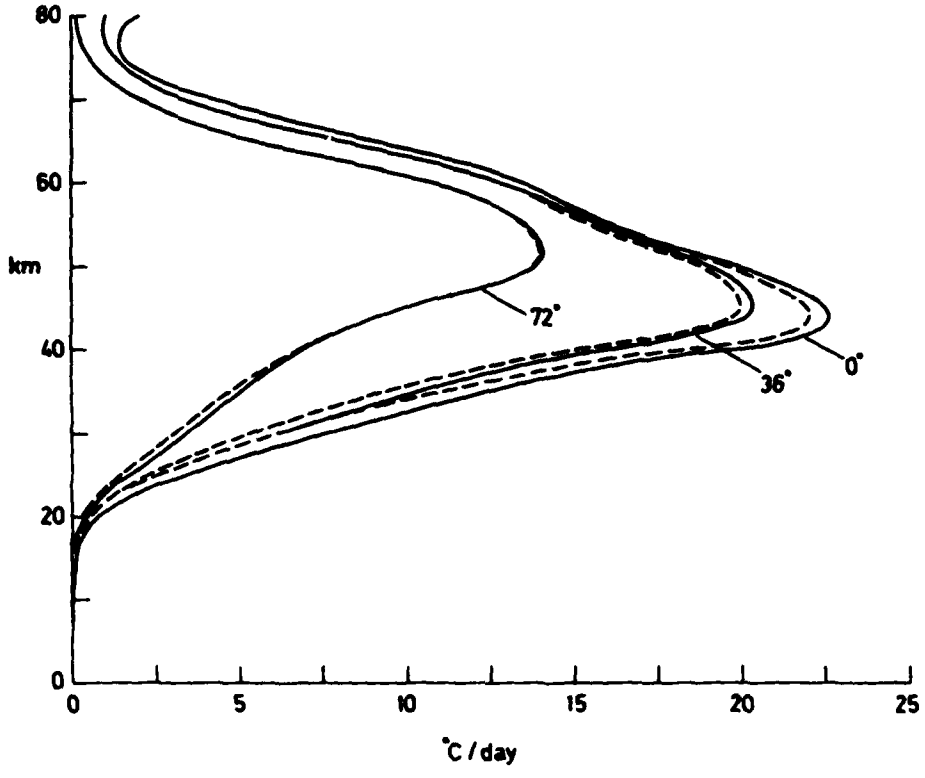


Fig. 1 Height profiles of equatorial heating rates for April ozone values. Solar zenith angles are marked on curves. Key: - - - - clear sky; ——— cloudy sky.

scattering and the Earth's surface for which an albedo of 0.14 is taken.

(ii) 100 per cent cloud with an albedo of 0.60 which in conjunction with the Earth's surface albedo of 0.14 gives a total albedo of 0.62 by (2.9).

For an overhead Sun, a maximum heating rate of nearly 23°C/day is obtained at 44 km (Fig. 1), which is in close agreement with previous calculations for equatorial conditions (Lacis and Hansen, 1974). The presence of clouds has a relatively large effect at lower heights (Fig. 1), e.g. at 20 km reflexion from clouds increases the heating rate by 46 per cent and at 30 km the increase is 20 per cent; but at greater heights heating by incoming UV radiation dominates that by reflected radiation which has traversed longer absorption paths and is at visual wavelengths.

Mean heating rates $J_o^o/c_p$ have been calculated by (3.20) for 0° solar declination (and April ozone and air densities) and are shown in Fig. 2 at various N latitudes for case (i) of clear skies. From Fig. 2 it is noted that the highest heating rate occurs at 30° N latitude and that at heights close to 50 km even 60° N heating rates may exceed equatorial values. Such results would appear to be a consequence of the decrease in ozone concentrations towards low latitudes that is found at 40-50 km in April (Table 1). The

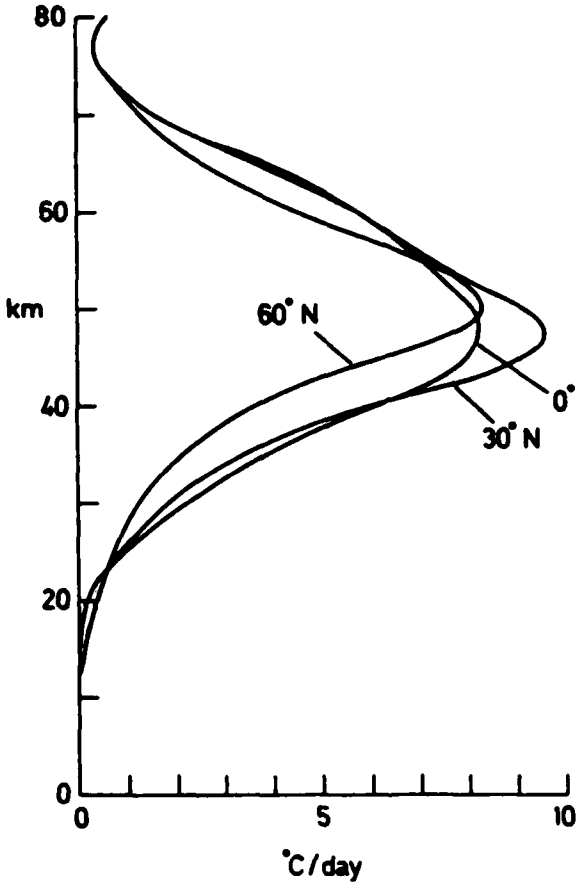


Fig. 2 Height profiles of mean heating rate, $J_o^o/c_p$, at different latitudes for April ozone and air density values and $0^o$ solar declination with no clouds.

observational evidence at 45 km for this decrease is shown in Fig. 3, where the continuous line corresponds to the values of Table 1. The low latitude ozone minimum is found in back-scatter UV spectrometer observations from the Nimbus 4 and OGO-4 satellites and has some support from the rather scattered assemblage of Umkehr results.

6.2 Diurnal Hough components

Diurnal Hough components of the heating rate have been calculated from (3.21) for the ozone and air density models described in § 4 and the reflectivity data of § 5. Normalized Hough functions are obtained as solutions of Laplace's tidal equation, methods of solving which have previously been reviewed (Groves, 1979). Diurnal Hough functions for s = 1 have previously been presented graphically (Groves, 1975), but may differ in sign from those used here which are positive at the equator if equatorially symmetric or increase at the equator with latitude if equatorially asymmetric.

With s = m = 1, it follows from (3.23) that $C_0$, $C_1$, $C_2$ are real; and hence by (3.22) that $J^1_{1,n}$ is real provided $f_0$, $f_1$, $f_2$ are real. By (3.17) to (3.19), $f_0$, $f_1$, $f_2$ are real if the daily variation in ozone concentration is symmetric with respect to local noon, but as described in § 4 the daily ozone variation is in general asymmetric with

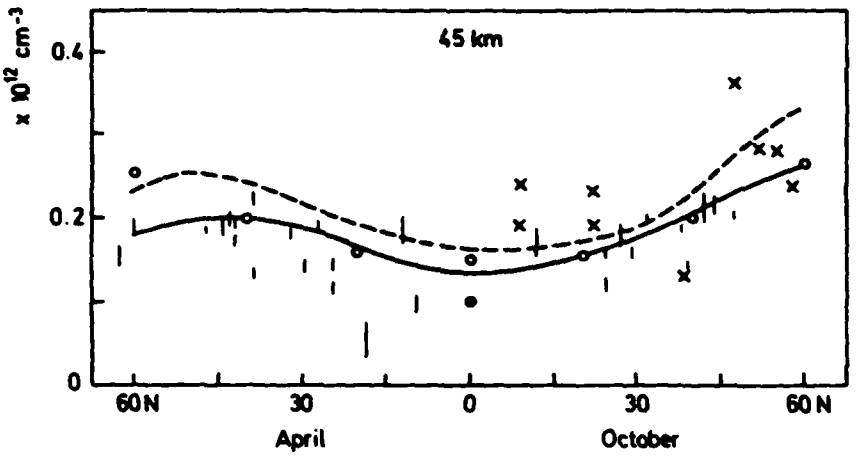


Fig. 3 Ozone concentrations at 45 km altitude for April and October from 0 to 60 N latitude. Key: o Nimbus 4 BUV spectrometer (Krueger et al., 1973); x Arcas optical ozonosonde (Krueger,1973); • OGO-4 BUV spectrometer (Anderson et al., 1969); - - - - OGO-4 BUV spectrometer (London et al., 1977); ——— model values (Table 1). Vertical lines refer to Umkehr determinations and extend to one standard deviation from the mean. Seasonal symmetry is assumed between N and S hemispheres (Lucas, 1978).

respect to local noon above 50 km and $J^1_{1,n}$ then has an imaginary part. When calculated, however, imaginary parts are very small (of order $10^{-3}$) relative to real parts and will therefore be neglected.

The results obtained for the three symmetric Hough components of heating $J^1_{1,1}$, $J^1_{1,3}$, $J^1_{1,5}$ are shown in Fig. 4, and those obtained for $J^1_{1,-2}$, $J^1_{1,-4}$, $J^1_{1,-6}$ which are symmetric components that are strongly affected by high-latitude heating are shown in Fig. 5. Values of solar declination and Sun-Earth distance have been taken for the middle day of each of the months January, April, July and October. In all cases July components are less than January components by about 7 per cent due to the increase in Sun-Earth distance, but April values are notably different from solstitial values. In Fig. 4, the minima in April components at 48 km would appear to arise from the shape of the latitudinal profile of the Hough function in relation to that of the heating which decreases towards low latitudes as discussed above ( § 6.1). The differences between solstitial and April values in Fig. 5 are again most likely to relate to changes in the ozone distribution: in the case of the $J^1_{1,-2}$ component the April values are actually higher, probably as a consequence of the form of $\Theta'_{1,-2}$ which unlike that for other modes considered has the same sign at all latitudes. The results plotted in Figs. 4 and 5 are given in Table 3 together with the October

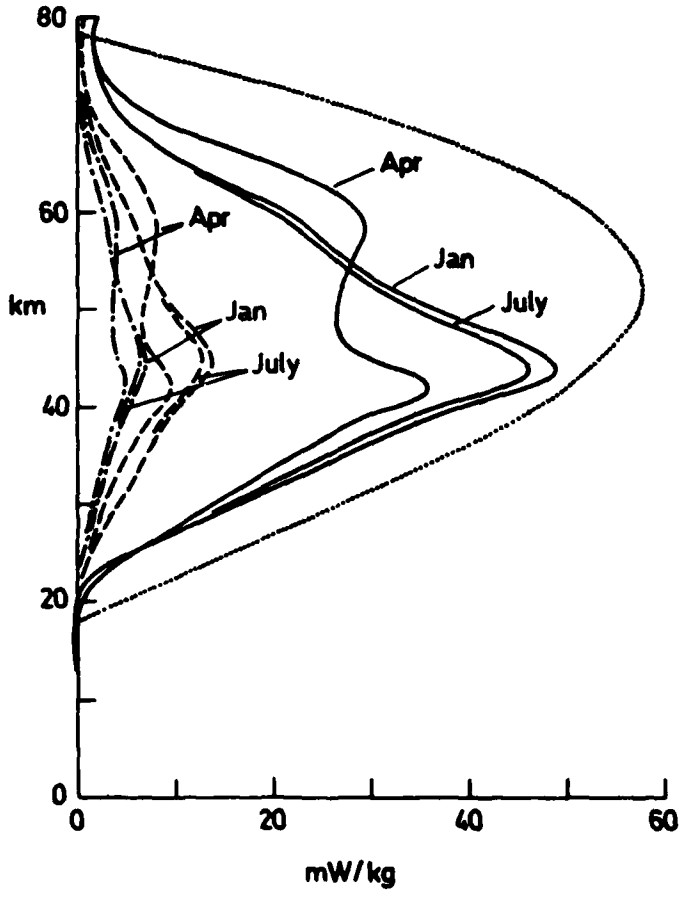


Fig. 4 Height profiles of Hough components of heating $J^1_{1,n}$ for n = 1,3,5. Key: —— $(-)J^1_{1,1}$; - - - - $J^1_{1,3}$; —·—·— $(-)J^1_{1,5}$; ..... $(-)J^1_{1,1}$ from Lindzen (1967).

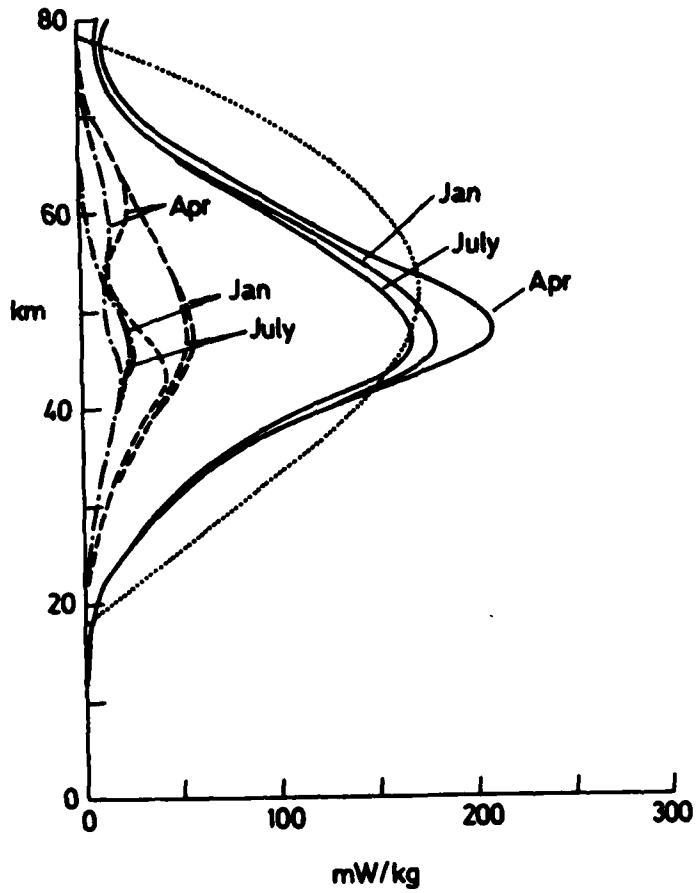


Fig. 5 Height profiles of Hough components of heating $J^1_{1,n}$ for n = -2, -4, -6. Key: ——— $(-)J^1_{1,-2}$; - - - - $(-)J^1_{1,-4}$; ·— ·— · $(-)J^1_{1,-6}$; ····· $(-)J^1_{1,-2}$ from Lindzen (1967).

values which hardly differ from the corresponding April values. Also shown on Figs. 4 and 5 respectively are $J^1_{1,1}$ and $J^1_{1,-2}$ taken from the earlier evaluation of Lindzen (1967). The new values are considerably lower than the earlier values at heights below and above the region of maximum heating.

The largest asymmetric Hough component of heating is $J^1_{1,-1}$ which is plotted in Fig. 6 for January and October together with the earlier evaluation of Lindzen (1967). Negative values arise in the mesosphere in January when N hemisphere ozone densities are considerably higher than S hemisphere values (Table 1) leading to greater heating in spite of the lower wintertime flux of incident solar radiation. In the stratosphere in January the asymmetry in ozone is much reduced (Table 1) and the heating asymmetry conforms with that of the solar flux. Likewise the asymmetry of the October heating accords with that of the radiational flux, the solar declination being $-8^o$: the October asymmetry in the stratosphere increases with the seasonal advance until the January profile is reached while in the mesosphere it reverses. July and April profiles are similar to those shown for January and October with a reversal of sign. The higher order $J^1_{1,-3}$, $J^1_{1,-5}$ components attain maximum values of 17 and 9 mW/kg respectively and are given in Table 3 whereas the asymmetric components $J^1_{1,2}$ and $J^1_{1,4}$ are less than 2 and 1 mW/kg respectively and are not included.

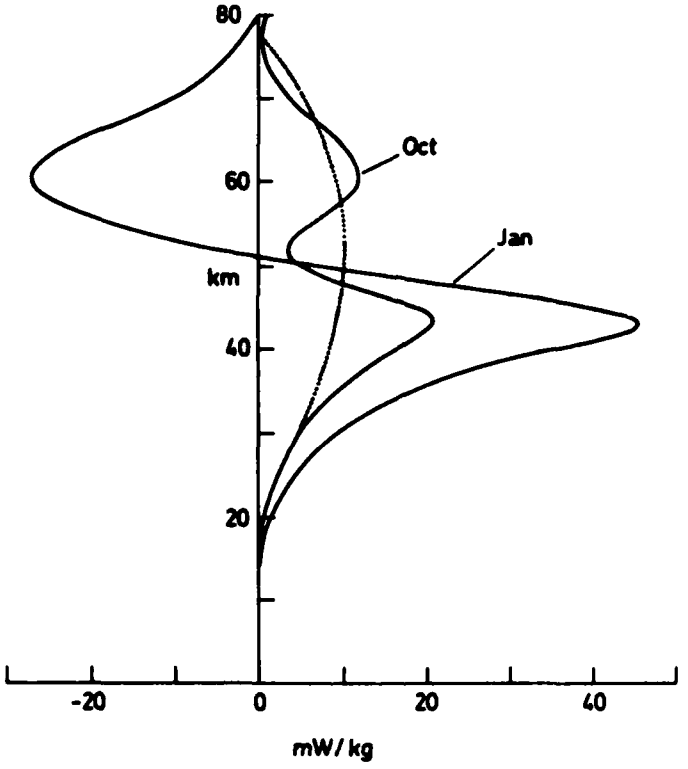


Fig. 6 Height profiles of the $J^1_{1,-1}$ component of heating. Key: ——— present calculations, ..... N hemisphere winter solstice from Lindzen (1967).

| H | (1,1,1) | | | | (1,1,3) | | | |
|---|---|---|---|---|---|---|---|---|
| km | mW/kg | | | | mW/kg | | | |
| | Jan | Apr | Jul | Oct | Jan | Apr | Jul | Oct |
| 0 | -0.0 | -0.0 | -0.0 | -0.0 | -0.0 | 0.0 | 0.0 | 0.0 |
| 2 | -0.0 | -0.0 | -0.0 | -0.0 | 0.0 | 0.0 | 0.0 | 0.0 |
| 4 | -0.0 | -0.0 | -0.0 | -0.0 | 0.0 | 0.0 | 0.0 | 0.0 |
| 6 | -0.0 | -0.0 | -0.0 | -0.0 | 0.0 | 0.0 | 0.0 | 0.0 |
| 8 | 0.0 | -0.0 | 0.0 | -0.0 | -0.0 | -0.0 | -0.0 | 0.0 |
| 10 | 0.1 | -0.0 | 0.0 | -0.0 | -0.0 | -0.0 | -0.0 | -0.0 |
| 12 | 0.1 | 0.1 | 0.1 | 0.1 | -0.0 | -0.0 | -0.0 | -0.0 |
| 14 | 0.2 | 0.1 | 0.2 | 0.1 | -0.1 | -0.1 | -0.1 | -0.1 |
| 16 | 0.3 | 0.2 | 0.2 | 0.2 | -0.1 | -0.1 | -0.1 | -0.1 |
| 18 | 0.3 | 0.1 | 0.3 | 0.1 | -0.1 | -0.1 | -0.1 | -0.1 |
| 20 | 0.1 | -0.6 | 0.0 | -0.6 | 0.0 | 0.0 | 0.1 | 0.1 |
| 22 | -1.0 | -1.9 | -1.0 | -2.0 | 0.4 | 0.4 | 0.4 | 0.5 |
| 24 | -3.4 | -4.1 | -3.3 | -4.3 | 0.9 | 0.9 | 0.9 | 1.2 |
| 26 | -7.4 | -7.1 | -7.1 | -7.3 | 1.8 | 1.6 | 1.8 | 1.9 |
| 28 | -12.0 | -10.4 | -11.4 | -10.6 | 2.9 | 2.3 | 2.9 | 2.7 |
| 30 | -16.6 | -13.7 | -15.7 | -14.0 | 4.2 | 2.8 | 4.1 | 3.3 |
| 32 | -20.8 | -17.1 | -19.7 | -17.5 | 5.2 | 3.7 | 5.0 | 4.1 |
| 34 | -25.1 | -20.9 | -23.7 | -21.3 | 6.3 | 4.7 | 6.0 | 5.1 |
| 36 | -29.2 | -24.1 | -27.5 | -24.5 | 7.3 | 5.7 | 7.0 | 6.2 |
| 38 | -33.4 | -27.2 | -31.5 | -27.7 | 8.5 | 6.7 | 8.1 | 7.1 |
| 40 | -38.9 | -32.5 | -36.5 | -33.0 | 10.0 | 8.3 | 9.4 | 8.7 |
| 42 | -46.6 | -35.9 | -43.6 | -36.4 | 12.3 | 9.8 | 11.6 | 10.2 |
| 44 | -49.0 | -32.2 | -46.0 | -32.5 | 13.6 | 8.9 | 12.8 | 9.2 |
| 46 | -46.2 | -27.9 | -43.5 | -28.1 | 13.1 | 7.4 | 12.3 | 7.6 |
| 48 | -41.4 | -26.2 | -39.0 | -26.3 | 11.6 | 6.7 | 10.9 | 6.9 |
| 50 | -36.2 | -26.4 | -34.1 | -26.6 | 9.9 | 6.7 | 9.3 | 6.9 |
| 52 | -32.2 | -27.0 | -30.3 | -27.2 | 8.5 | 7.1 | 8.0 | 7.3 |
| 54 | -28.9 | -27.7 | -27.2 | -28.0 | 7.4 | 7.5 | 7.0 | 7.7 |
| 56 | -26.5 | -28.8 | -25.0 | -29.1 | 6.7 | 7.9 | 6.3 | 8.1 |
| 58 | -24.0 | -29.3 | -22.7 | -29.6 | 6.0 | 8.1 | 5.7 | 8.2 |
| 60 | -21.1 | -28.7 | -19.9 | -29.0 | 5.3 | 7.9 | 5.0 | 8.0 |
| 62 | -16.9 | -26.1 | -15.9 | -26.4 | 4.2 | 7.1 | 4.0 | 7.2 |
| 64 | -12.8 | -22.0 | -12.0 | -22.3 | 3.2 | 5.9 | 3.0 | 6.0 |
| 66 | -9.1 | -16.9 | -8.6 | -17.1 | 2.3 | 4.4 | 2.1 | 4.5 |
| 68 | -6.3 | -11.8 | -5.9 | -12.0 | 1.6 | 3.0 | 1.5 | 3.0 |
| 70 | -4.3 | -7.7 | -4.1 | -7.8 | 1.1 | 1.9 | 1.0 | 1.9 |
| 72 | -3.1 | -4.4 | -2.9 | -4.4 | 0.8 | 1.0 | 0.7 | 1.1 |
| 74 | -2.3 | -2.7 | -2.2 | -2.7 | 0.6 | 0.6 | 0.6 | 0.6 |
| 76 | -1.9 | -1.9 | -1.8 | -1.9 | 0.5 | 0.4 | 0.5 | 0.4 |
| 78 | -1.9 | -2.0 | -1.8 | -2.0 | 0.5 | 0.4 | 0.5 | 0.4 |
| 80 | -2.2 | -3.3 | -2.1 | -3.3 | 0.6 | 0.7 | 0.5 | 0.7 |

Table 3. Hough components of ozone heating $J^{s}_{m,n}$ associated with mode (m,s,n)

| H | (1,1,5) | | | | (1,1,-1) | | | |
|---|---|---|---|---|---|---|---|---|
| km | mW/kg | | | | mW/kg | | | |
| | Jan | Apr | Jul | Oct | Jan | Apr | Jul | Oct |
| 0 | -0.0 | -0.0 | -0.0 | -0.0 | 0.0 | -0.0 | -0.0 | 0.0 |
| 2 | -0.0 | -0.0 | -0.0 | -0.0 | 0.0 | -0.0 | -0.0 | 0.0 |
| 4 | -0.0 | 0.0 | -0.0 | -0.0 | 0.0 | -0.0 | -0.0 | 0.0 |
| 6 | -0.0 | 0.0 | -0.0 | 0.0 | 0.0 | -0.1 | -0.0 | 0.1 |
| 8 | 0.0 | 0.0 | 0.0 | 0.0 | 0.1 | -0.1 | -0.1 | 0.1 |
| 10 | 0.0 | 0.0 | 0.0 | 0.0 | 0.1 | -0.2 | -0.1 | 0.2 |
| 12 | 0.0 | 0.0 | 0.0 | 0.0 | 0.1 | -0.3 | -0.1 | 0.3 |
| 14 | 0.0 | 0.0 | 0.0 | 0.0 | 0.1 | -0.5 | -0.1 | 0.4 |
| 16 | 0.0 | 0.1 | 0.0 | 0.1 | 0.3 | -0.7 | -0.3 | 0.7 |
| 18 | 0.1 | 0.1 | 0.0 | 0.1 | 0.7 | -1.1 | -0.6 | 1.0 |
| 20 | -0.0 | -0.0 | -0.0 | -0.0 | 1.5 | -1.5 | -1.4 | 1.4 |
| 22 | -0.1 | -0.2 | -0.1 | -0.2 | 2.5 | -2.0 | -2.3 | 2.0 |
| 24 | -0.4 | -0.4 | -0.4 | -0.5 | 3.8 | -2.6 | -3.4 | 2.5 |
| 26 | -0.9 | -0.8 | -0.8 | -0.8 | 5.3 | -3.1 | -4.7 | 3.1 |
| 28 | -1.4 | -1.2 | -1.3 | -1.2 | 7.1 | -3.8 | -6.5 | 3.8 |
| 30 | -2.0 | -1.5 | -1.9 | -1.6 | 9.3 | -4.6 | -8.5 | 4.6 |
| 32 | -2.5 | -1.9 | -2.3 | -2.0 | 12.5 | -6.4 | -11.5 | 6.2 |
| 34 | -3.1 | -2.4 | -2.9 | -2.5 | 16.7 | -8.7 | -15.5 | 8.4 |
| 36 | -3.7 | -3.0 | -3.4 | -3.0 | 21.7 | -11.6 | -20.3 | 11.0 |
| 38 | -4.3 | -3.5 | -4.0 | -3.6 | 27.0 | -14.6 | -25.4 | 13.6 |
| 40 | -5.1 | -4.2 | -4.7 | -4.3 | 35.2 | -18.0 | -33.2 | 16.4 |
| 42 | -6.2 | -5.0 | -5.8 | -5.1 | 44.4 | -21.9 | -42.1 | 19.5 |
| 44 | -6.8 | -4.7 | -6.4 | -4.7 | 43.9 | -23.5 | -41.7 | 20.4 |
| 46 | -6.6 | -3.9 | -6.2 | -4.0 | 33.7 | -19.4 | -32.2 | 16.1 |
| 48 | -5.8 | -3.6 | -5.5 | -3.6 | 20.1 | -12.8 | -19.4 | 9.8 |
| 50 | -5.0 | -3.6 | -4.7 | -3.6 | 6.5 | -7.6 | -6.8 | 5.1 |
| 52 | -4.3 | -3.7 | -4.0 | -3.7 | -5.1 | -5.6 | 4.1 | 3.8 |
| 54 | -3.8 | -3.8 | -3.6 | -3.9 | -14.2 | -6.2 | 12.7 | 5.1 |
| 56 | -3.4 | -4.0 | -3.2 | -4.0 | -20.8 | -8.7 | 19.0 | 8.1 |
| 58 | -3.1 | -4.0 | -2.9 | -4.1 | -25.2 | -10.9 | 23.1 | 10.7 |
| 60 | -2.7 | -3.9 | -2.6 | -3.9 | -27.0 | -12.1 | 24.9 | 12.0 |
| 62 | -2.2 | -3.5 | -2.0 | -3.6 | -26.4 | -11.7 | 24.4 | 11.7 |
| 64 | -1.6 | -2.9 | -1.5 | -3.0 | -23.5 | -10.3 | 21.7 | 10.3 |
| 66 | -1.2 | -2.2 | -1.1 | -2.3 | -19.1 | -8.1 | 17.7 | 8.1 |
| 68 | -0.8 | -1.5 | -0.8 | -1.6 | -14.3 | -5.8 | 13.3 | 5.7 |
| 70 | -0.6 | -1.0 | -0.5 | -1.0 | -10.1 | -3.8 | 9.4 | 3.8 |
| 72 | -0.4 | -0.6 | -0.4 | -0.6 | -6.6 | -2.2 | 6.1 | 2.1 |
| 74 | -0.3 | -0.3 | -0.3 | -0.3 | -4.2 | -1.3 | 3.8 | 1.2 |
| 76 | -0.3 | -0.2 | -0.2 | -0.2 | -2.5 | -0.8 | 2.3 | 0.7 |
| 78 | -0.3 | -0.2 | -0.2 | -0.2 | -1.3 | -0.7 | 1.1 | 0.6 |
| 80 | -0.3 | -0.4 | -0.3 | -0.4 | 0.0 | -1.1 | -0.0 | 1.1 |

Table 3. (continued)

| H | (1,1,-2) | | | | (1,1,-3) | | | |
|---|---|---|---|---|---|---|---|---|
| km | mW/kg | | | | mW/kg | | | |
| | Jan | Apr | Jul | Oct | Jan | Apr | Jul | Oct |
| 0 | -0.1 | -0.1 | -0.1 | -0.1 | -0.0 | 0.0 | 0.0 | -0.0 |
| 2 | -0.1 | -0.1 | -0.1 | -0.1 | -0.0 | 0.0 | 0.0 | -0.0 |
| 4 | -0.1 | -0.1 | -0.1 | -0.1 | -0.0 | 0.0 | 0.0 | -0.0 |
| 6 | -0.2 | -0.2 | -0.2 | -0.2 | -0.0 | 0.0 | 0.0 | -0.0 |
| 8 | -0.3 | -0.4 | -0.3 | -0.4 | -0.0 | 0.1 | 0.0 | -0.1 |
| 10 | -0.5 | -0.6 | -0.5 | -0.6 | -0.1 | 0.2 | 0.1 | -0.1 |
| 12 | -0.7 | -0.9 | -0.7 | -0.9 | -0.1 | 0.2 | 0.2 | -0.1 |
| 14 | -1.0 | -1.3 | -1.0 | -1.3 | -0.3 | 0.4 | 0.3 | -0.2 |
| 16 | -1.6 | -2.1 | -1.5 | -2.1 | -0.4 | 0.5 | 0.5 | -0.3 |
| 18 | -2.9 | -3.7 | -2.7 | -3.7 | -0.6 | 0.7 | 0.7 | -0.3 |
| 20 | -5.6 | -6.8 | -5.2 | -6.9 | -0.7 | 0.9 | 0.8 | -0.5 |
| 22 | -10.0 | -11.4 | -9.3 | -11.6 | -0.6 | 1.1 | 0.8 | -0.6 |
| 24 | -16.6 | -18.1 | -15.5 | -18.5 | -0.6 | 1.4 | 0.8 | -0.7 |
| 26 | -25.0 | -26.0 | -23.2 | -26.6 | -0.6 | 1.6 | 0.9 | -1.0 |
| 28 | -33.8 | -34.2 | -31.4 | -35.1 | -0.7 | 1.9 | 1.0 | -1.3 |
| 30 | -42.6 | -42.6 | -39.7 | -43.8 | -1.0 | 2.3 | 1.3 | -1.7 |
| 32 | -53.4 | -53.7 | -49.8 | -55.1 | -1.3 | 2.7 | 1.7 | -2.2 |
| 34 | -66.4 | -67.4 | -61.9 | -69.0 | -1.9 | 3.3 | 2.2 | -2.7 |
| 36 | -81.7 | -83.7 | -76.2 | -85.5 | -2.9 | 4.1 | 3.1 | -3.4 |
| 38 | -99.7 | -103.0 | -93.0 | -105.1 | -4.4 | 5.1 | 4.5 | -4.3 |
| 40 | -123.0 | -127.0 | -114.8 | -129.5 | -5.7 | 6.1 | 5.6 | -5.1 |
| 42 | -151.7 | -156.8 | -141.5 | -159.7 | -7.0 | 7.0 | 6.9 | -5.8 |
| 44 | -172.6 | -185.9 | -161.0 | -189.4 | -11.2 | 10.4 | 10.6 | -8.6 |
| 46 | -181.0 | -204.9 | -168.7 | -209.0 | -15.3 | 14.7 | 14.4 | -12.1 |
| 48 | -181.1 | -211.6 | -168.6 | -216.1 | -17.5 | 15.5 | 16.4 | -12.6 |
| 50 | -173.4 | -204.3 | -161.4 | -208.7 | -16.8 | 13.7 | 15.8 | -10.5 |
| 52 | -162.6 | -186.9 | -151.2 | -190.9 | -14.2 | 10.1 | 13.5 | -7.3 |
| 54 | -148.7 | -165.1 | -138.3 | -168.5 | -10.7 | 8.2 | 10.3 | -6.5 |
| 56 | -134.5 | -143.9 | -125.1 | -146.6 | -7.5 | 8.6 | 7.3 | -7.8 |
| 58 | -119.2 | -125.0 | -110.9 | -127.2 | -4.8 | 8.8 | 4.8 | -8.6 |
| 60 | -102.6 | -107.9 | -95.6 | -109.7 | -2.8 | 7.9 | 2.9 | -8.0 |
| 62 | -83.1 | -91.7 | -77.4 | -93.1 | -1.4 | 6.3 | 1.6 | -6.3 |
| 64 | -64.8 | -75.4 | -60.4 | -76.5 | -0.5 | 4.8 | 0.7 | -4.8 |
| 66 | -48.2 | -58.8 | -44.9 | -59.7 | 0.0 | 3.7 | 0.1 | -3.8 |
| 68 | -34.8 | -43.5 | -32.4 | -44.2 | 0.2 | 3.1 | -0.1 | -3.1 |
| 70 | -24.7 | -31.4 | -23.0 | -31.9 | 0.3 | 2.5 | -0.2 | -2.5 |
| 72 | -17.3 | -21.4 | -16.1 | -21.8 | 0.1 | 1.8 | -0.0 | -1.8 |
| 74 | -12.8 | -15.9 | -12.0 | -16.2 | -0.0 | 1.3 | 0.1 | -1.2 |
| 76 | -10.3 | -13.1 | -9.6 | -13.4 | -0.1 | 0.9 | 0.1 | -0.8 |
| 78 | -9.6 | -13.5 | -9.0 | -13.7 | -0.2 | 0.8 | 0.2 | -0.7 |
| 80 | -11.1 | -17.9 | -10.3 | -18.3 | -0.3 | 1.0 | 0.3 | -0.9 |

Table 3. (continued)

| H | (1,1,-4) | | | | (1,1,-5) | | | |
|---|---|---|---|---|---|---|---|---|
| km | mW/kg | | | | mW/kg | | | |
| | Jan | Apr | Jul | Oct | Jan | Apr | Jul | Oct |
| 0 | -0.0 | -0.0 | -0.0 | -0.0 | -0.0 | 0.0 | 0.0 | -0.0 |
| 2 | -0.0 | -0.0 | -0.0 | -0.0 | -0.0 | 0.0 | 0.0 | -0.0 |
| 4 | -0.0 | -0.0 | -0.0 | -0.0 | -0.0 | 0.0 | 0.0 | -0.0 |
| 6 | -0.0 | 0.0 | -0.0 | -0.0 | -0.0 | 0.0 | 0.0 | -0.0 |
| 8 | -0.0 | 0.0 | -0.0 | -0.0 | -0.0 | 0.0 | 0.0 | -0.0 |
| 10 | -0.0 | 0.1 | -0.0 | 0.0 | -0.0 | 0.0 | 0.0 | -0.1 |
| 12 | 0.0 | 0.2 | 0.0 | 0.1 | -0.1 | 0.0 | 0.0 | -0.1 |
| 14 | 0.2 | 0.4 | 0.2 | 0.3 | -0.1 | -0.0 | 0.1 | -0.1 |
| 16 | 0.3 | 0.7 | 0.3 | 0.5 | -0.1 | -0.1 | 0.1 | -0.0 |
| 18 | 0.2 | 0.8 | 0.3 | 0.6 | -0.1 | -0.2 | 0.1 | 0.0 |
| 20 | -0.5 | 0.4 | -0.3 | 0.1 | -0.1 | -0.2 | 0.1 | 0.1 |
| 22 | -2.0 | -0.9 | -1.7 | -1.3 | -0.1 | -0.2 | 0.1 | 0.1 |
| 24 | -4.9 | -3.3 | -4.3 | -3.8 | -0.1 | -0.1 | 0.1 | -0.0 |
| 26 | -8.6 | -6.4 | -7.8 | -6.9 | -0.2 | -0.0 | 0.3 | -0.1 |
| 28 | -12.3 | -9.3 | -11.2 | -9.8 | -0.4 | 0.1 | 0.4 | -0.2 |
| 30 | -15.7 | -12.1 | -14.4 | -12.6 | -0.7 | 0.1 | 0.7 | -0.1 |
| 32 | -19.6 | -15.8 | -18.0 | -16.3 | -0.9 | 0.1 | 0.9 | -0.1 |
| 34 | -23.8 | -20.1 | -22.0 | -20.6 | -1.2 | 0.1 | 1.2 | -0.2 |
| 36 | -28.3 | -24.6 | -26.2 | -25.3 | -1.6 | -0.0 | 1.5 | -0.0 |
| 38 | -33.4 | -29.2 | -30.9 | -29.8 | -1.8 | -0.5 | 1.8 | 0.4 |
| 40 | -39.8 | -34.7 | -37.0 | -35.3 | -1.7 | -1.5 | 1.7 | 1.5 |
| 42 | -48.4 | -41.8 | -45.0 | -42.4 | -1.7 | -2.3 | 1.8 | 2.3 |
| 44 | -54.2 | -44.2 | -50.5 | -44.7 | -2.5 | -2.1 | 2.5 | 2.2 |
| 46 | -56.4 | -38.6 | -52.8 | -38.5 | -3.2 | -4.2 | 3.3 | 4.4 |
| 48 | -56.4 | -29.7 | -53.0 | -28.8 | -3.5 | -8.4 | 3.7 | 8.4 |
| 50 | -54.2 | -22.1 | -51.1 | -20.0 | -3.4 | -9.5 | 3.8 | 8.8 |
| 52 | -50.8 | -15.8 | -48.0 | -13.3 | -2.5 | -7.6 | 3.0 | 6.6 |
| 54 | -46.5 | -14.3 | -44.0 | -12.3 | -0.9 | -5.2 | 1.4 | 4.6 |
| 56 | -42.5 | -17.9 | -40.1 | -16.6 | 1.4 | -3.7 | -0.8 | 3.5 |
| 58 | -37.6 | -22.3 | -35.5 | -21.6 | 4.1 | -2.6 | -3.4 | 2.6 |
| 60 | -32.0 | -24.8 | -30.3 | -24.5 | 6.1 | -1.7 | -5.4 | 1.8 |
| 62 | -25.2 | -24.5 | -23.8 | -24.5 | 6.9 | -0.8 | -6.2 | 0.9 |
| 64 | -19.0 | -21.8 | -17.9 | -21.8 | 6.7 | -0.3 | -6.0 | 0.4 |
| 66 | -13.5 | -16.9 | -12.8 | -17.0 | 5.8 | -0.3 | -5.2 | 0.3 |
| 68 | -9.4 | -11.5 | -8.9 | -11.5 | 4.5 | -0.5 | -4.1 | 0.5 |
| 70 | -6.5 | -6.9 | -6.2 | -6.9 | 3.3 | -0.7 | -3.0 | 0.7 |
| 72 | -4.6 | -3.1 | -4.3 | -3.0 | 2.2 | -0.8 | -2.0 | 0.7 |
| 74 | -3.4 | -1.0 | -3.3 | -0.9 | 1.5 | -0.8 | -1.3 | 0.8 |
| 76 | -2.8 | 0.2 | -2.6 | 0.4 | 1.0 | -0.8 | -0.9 | 0.7 |
| 78 | -2.6 | 0.4 | -2.4 | 0.6 | 0.7 | -0.8 | -0.7 | 0.7 |
| 80 | -2.9 | -0.6 | -2.8 | -0.4 | 0.6 | -0.8 | -0.5 | 0.8 |

Table 3. (continued)

| H | (1,1,-6) | | | | (2,2,2) | | | |
|---|---|---|---|---|---|---|---|---|
| km | mW/kg | | | | mW/kg | | | |
| | Jan | Apr | Jul | Oct | Jan | Apr | Jul | Oct |
| 0 | 0.0 | -0.0 | 0.0 | -0.0 | 0.0 | 0.0 | 0.0 | 0.0 |
| 2 | 0.0 | -0.0 | 0.0 | 0.0 | 0.0 | 0.0 | 0.0 | 0.0 |
| 4 | 0.0 | -0.0 | 0.0 | 0.0 | 0.0 | 0.0 | 0.0 | 0.0 |
| 6 | 0.0 | 0.0 | 0.0 | 0.0 | 0.0 | 0.0 | 0.0 | 0.0 |
| 8 | 0.0 | 0.0 | 0.0 | 0.0 | 0.1 | 0.1 | 0.1 | 0.1 |
| 10 | 0.1 | 0.0 | 0.1 | 0.0 | 0.1 | 0.1 | 0.1 | 0.1 |
| 12 | 0.2 | 0.1 | 0.1 | 0.1 | 0.1 | 0.1 | 0.1 | 0.1 |
| 14 | 0.3 | 0.1 | 0.2 | 0.1 | 0.1 | 0.2 | 0.1 | 0.2 |
| 16 | 0.4 | 0.1 | 0.3 | 0.2 | 0.2 | 0.3 | 0.2 | 0.3 |
| 18 | 0.5 | 0.0 | 0.4 | 0.1 | 0.4 | 0.6 | 0.4 | 0.6 |
| 20 | 0.3 | -0.3 | 0.2 | -0.2 | 1.1 | 1.4 | 1.0 | 1.5 |
| 22 | -0.2 | -0.9 | -0.3 | -0.9 | 2.3 | 2.7 | 2.1 | 2.9 |
| 24 | -1.4 | -2.1 | -1.4 | -2.2 | 4.4 | 4.9 | 4.1 | 5.1 |
| 26 | -3.1 | -3.6 | -3.0 | -3.7 | 7.3 | 7.6 | 6.9 | 7.9 |
| 28 | -5.0 | -5.1 | -4.7 | -5.2 | 10.7 | 10.6 | 10.0 | 11.0 |
| 30 | -6.7 | -6.3 | -6.3 | -6.5 | 14.4 | 14.0 | 13.5 | 14.5 |
| 32 | -8.4 | -8.0 | -8.0 | -8.3 | 18.9 | 18.5 | 17.7 | 19.1 |
| 34 | -10.4 | -10.0 | -9.8 | -10.3 | 24.6 | 24.2 | 22.9 | 24.9 |
| 36 | -12.6 | -12.2 | -11.8 | -12.5 | 30.8 | 30.5 | 28.8 | 31.3 |
| 38 | -15.2 | -14.5 | -14.3 | -14.8 | 37.6 | 37.4 | 35.0 | 38.3 |
| 40 | -18.3 | -17.4 | -17.2 | -17.8 | 47.3 | 47.5 | 44.2 | 48.5 |
| 42 | -22.3 | -20.7 | -20.9 | -21.1 | 59.5 | 58.8 | 55.5 | 60.0 |
| 44 | -25.7 | -20.3 | -24.2 | -20.7 | 62.9 | 62.4 | 58.7 | 63.5 |
| 46 | -26.3 | -17.1 | -24.8 | -17.1 | 56.3 | 56.9 | 52.5 | 57.9 |
| 48 | -23.7 | -13.6 | -22.4 | -13.8 | 46.8 | 47.6 | 43.7 | 48.4 |
| 50 | -18.8 | -12.4 | -18.0 | -13.5 | 38.1 | 38.6 | 35.6 | 39.2 |
| 52 | -13.3 | -13.3 | -13.0 | -14.9 | 30.5 | 29.8 | 28.5 | 30.3 |
| 54 | -8.8 | -14.6 | -8.8 | -15.9 | 24.8 | 23.3 | 23.1 | 23.7 |
| 56 | -6.3 | -15.3 | -6.5 | -16.3 | 21.5 | 19.7 | 20.1 | 20.0 |
| 58 | -4.9 | -15.6 | -5.1 | -16.3 | 20.1 | 18.4 | 18.9 | 18.8 |
| 60 | -3.7 | -15.3 | -3.9 | -15.8 | 19.3 | 18.2 | 18.0 | 18.6 |
| 62 | -2.2 | -13.8 | -2.4 | -14.2 | 17.7 | 18.1 | 16.6 | 18.4 |
| 64 | -0.9 | -11.7 | -1.1 | -11.9 | 15.4 | 17.0 | 14.4 | 17.3 |
| 66 | -0.0 | -9.1 | -0.2 | -9.3 | 12.4 | 14.6 | 11.6 | 14.8 |
| 68 | 0.3 | -6.6 | 0.1 | -6.7 | 9.5 | 11.5 | 8.9 | 11.7 |
| 70 | 0.3 | -4.5 | 0.2 | -4.7 | 7.2 | 8.7 | 6.7 | 8.8 |
| 72 | 0.1 | -2.8 | 0.0 | -2.9 | 5.5 | 6.2 | 5.2 | 6.3 |
| 74 | -0.1 | -1.9 | -0.1 | -2.0 | 4.4 | 4.7 | 4.1 | 4.8 |
| 76 | -0.3 | -1.5 | -0.3 | -1.7 | 3.7 | 3.9 | 3.4 | 3.9 |
| 78 | -0.4 | -1.6 | -0.4 | -1.7 | 3.3 | 3.9 | 3.1 | 3.9 |
| 80 | -0.5 | -2.1 | -0.5 | -2.3 | 3.1 | 4.4 | 2.9 | 4.5 |

Table 3. (continued)

| u | (2,2,3) | | | | (2,2,4) | | | |
|---|---|---|---|---|---|---|---|---|
| km | mW/kg | | | | mW/kg | | | |
| | Jan | Apr | Jul | Oct | Jan | Apr | Jul | Oct |
| 0 | 0.0 | -0.0 | -0.0 | 0.0 | -0.0 | -0.0 | -0.0 | -0.0 |
| 2 | 0.0 | -0.0 | -0.0 | 0.0 | -0.0 | -0.0 | -0.0 | -0.0 |
| 4 | 0.0 | -0.0 | -0.0 | 0.0 | -0.0 | -0.0 | -0.0 | -0.0 |
| 6 | 0.0 | -0.0 | -0.0 | 0.0 | -0.0 | -0.0 | -0.0 | -0.0 |
| 8 | 0.0 | -0.0 | -0.0 | 0.0 | -0.0 | -0.0 | -0.0 | -0.0 |
| 10 | 0.1 | -0.0 | -0.1 | 0.0 | -0.1 | -0.1 | -0.1 | -0.1 |
| 12 | 0.1 | -0.0 | -0.1 | -0.0 | -0.1 | -0.1 | -0.1 | -0.1 |
| 14 | 0.1 | 0.0 | -0.1 | -0.0 | -0.2 | -0.2 | -0.2 | -0.2 |
| 16 | 0.2 | 0.0 | -0.2 | -0.0 | -0.2 | -0.3 | -0.2 | -0.3 |
| 18 | 0.3 | -0.0 | -0.3 | -0.0 | -0.4 | -0.4 | -0.4 | -0.5 |
| 20 | 0.4 | -0.1 | -0.4 | 0.0 | -0.7 | -0.7 | -0.6 | -0.8 |
| 22 | 0.7 | -0.3 | -0.7 | 0.2 | -1.1 | -1.1 | -0.9 | -1.2 |
| 24 | 1.2 | -0.5 | -1.2 | 0.4 | -1.5 | -1.7 | -1.4 | -1.8 |
| 26 | 1.8 | -0.9 | -1.8 | 0.6 | -2.0 | -2.4 | -1.8 | -2.6 |
| 28 | 2.3 | -1.1 | -2.3 | 0.8 | -2.3 | -3.1 | -2.1 | -3.3 |
| 30 | 2.6 | -1.3 | -2.6 | 0.9 | -2.7 | -3.9 | -2.4 | -4.1 |
| 32 | 2.8 | -1.3 | -2.8 | 1.0 | -3.5 | -5.2 | -3.1 | -5.5 |
| 34 | 2.9 | -1.3 | -2.9 | 0.9 | -4.7 | -7.1 | -4.3 | -7.4 |
| 36 | 3.1 | -1.2 | -3.1 | 0.8 | -6.5 | -9.9 | -5.9 | -10.3 |
| 38 | 3.7 | -1.4 | -3.7 | 1.0 | -8.8 | -13.2 | -8.0 | -13.7 |
| 40 | 2.7 | -1.2 | -2.7 | 0.9 | -11.? | -16.5 | -10.9 | -17.1 |
| 42 | 2.8 | -1.3 | -2.8 | 1.0 | -15.5 | -23.3 | -14.2 | -24.0 |
| 44 | 10.2 | -3.8 | -9.7 | 3.3 | -18.6 | -31.4 | -17.0 | -32.4 |
| 46 | 20.7 | -8.1 | -19.6 | 7.1 | -20.2 | -33.7 | -18.4 | -34.7 |
| 48 | 28.0 | -11.3 | -26.5 | 10.0 | -20.0 | -29.4 | -18.3 | -30.3 |
| 50 | 30.8 | -12.2 | -29.1 | 10.8 | -18.6 | -22.8 | -17.1 | -23.4 |
| 52 | 31.2 | -11.7 | -29.6 | 10.3 | -16.6 | -16.2 | -15.2 | -16.6 |
| 54 | 29.8 | -10.6 | -28.2 | 9.2 | -14.8 | -11.3 | -13.7 | -11.6 |
| 56 | 27.4 | -9.2 | -26.0 | 7.9 | -13.9 | -8.2 | -12.9 | -8.5 |
| 58 | 24.3 | -7.7 | -23.1 | 6.6 | -13.7 | -6.7 | -12.8 | -7.0 |
| 60 | 21.0 | -6.1 | -19.9 | 5.2 | -13.3 | -6.0 | -12.4 | -6.2 |
| 62 | 17.3 | -4.7 | -16.4 | 3.9 | -12.4 | -5.7 | -11.6 | -5.9 |
| 64 | 13.7 | -3.4 | -13.0 | 2.8 | -10.8 | -5.3 | -10.1 | -5.5 |
| 66 | 10.4 | -2.4 | -9.9 | 1.9 | -8.7 | -4.7 | -8.1 | -4.9 |
| 68 | 7.6 | -1.6 | -7.2 | 1.3 | -6.6 | -3.9 | -6.2 | -4.1 |
| 70 | 5.4 | -1.1 | -5.1 | 0.9 | -4.9 | -3.2 | -4.6 | -3.3 |
| 72 | 3.7 | -0.7 | -3.5 | 0.6 | -3.5 | -2.6 | -3.3 | -2.7 |
| 74 | 2.6 | -0.5 | -2.5 | 0.4 | -2.6 | -2.2 | -2.4 | -2.3 |
| 76 | 1.9 | -0.4 | -1.8 | 0.4 | -2.0 | -2.0 | -1.9 | -2.0 |
| 78 | 1.5 | -0.4 | -1.4 | 0.4 | -1.7 | -1.9 | -1.6 | -2.0 |
| 80 | 1.5 | -0.7 | -1.4 | 0.6 | -1.4 | -2.0 | -1.3 | -2.1 |

Table 3. (continued)

| H | (2,2,5) | | | | (2,2,6) | | | |
|---|---|---|---|---|---|---|---|---|
| km | mW/kg | | | | mW/kg | | | |
| | Jan | Apr | Jul | Oct | Jan | Apr | Jul | Oct |
| 0 | -0.0 | 0.0 | 0.0 | 0.0 | 0.0 | 0.0 | 0.0 | 0.0 |
| 2 | -0.0 | 0.0 | 0.0 | 0.0 | 0.0 | 0.0 | 0.0 | 0.0 |
| 4 | -0.0 | 0.0 | 0.0 | 0.0 | 0.0 | 0.0 | 0.0 | 0.0 |
| 6 | -0.0 | 0.0 | 0.0 | 0.0 | 0.0 | 0.0 | 0.0 | 0.0 |
| 8 | -0.0 | 0.0 | 0.0 | 0.0 | 0.0 | 0.0 | 0.0 | 0.0 |
| 10 | -0.1 | 0.0 | 0.1 | 0.0 | 0.1 | 0.1 | 0.0 | 0.1 |
| 12 | -0.1 | 0.0 | 0.1 | 0.0 | 0.1 | 0.1 | 0.1 | 0.1 |
| 14 | -0.2 | 0.0 | 0.2 | -0.0 | 0.1 | 0.1 | 0.1 | 0.2 |
| 16 | -0.2 | 0.0 | 0.2 | -0.0 | 0.2 | 0.2 | 0.2 | 0.2 |
| 18 | -0.4 | 0.1 | 0.3 | -0.0 | 0.3 | 0.4 | 0.2 | 0.4 |
| 20 | -0.5 | 0.1 | 0.5 | -0.1 | 0.4 | 0.5 | 0.3 | 0.6 |
| 22 | -0.9 | 0.2 | 0.8 | -0.1 | 0.5 | 0.8 | 0.4 | 0.8 |
| 24 | -1.3 | 0.4 | 1.2 | -0.2 | 0.7 | 1.0 | 0.6 | 1.0 |
| 26 | -1.6 | 0.5 | 1.6 | -0.3 | 0.9 | 1.4 | 0.8 | 1.4 |
| 28 | -1.8 | 0.7 | 1.8 | -0.5 | 1.1 | 1.8 | 0.9 | 1.8 |
| 30 | -1.8 | 0.9 | 1.8 | -0.6 | 1.2 | 2.3 | 1.0 | 2.3 |
| 32 | -1.9 | 1.0 | 1.9 | -0.7 | 1.5 | 3.0 | 1.2 | 3.0 |
| 34 | -2.0 | 1.1 | 2.0 | -0.7 | 1.9 | 3.9 | 1.7 | 3.9 |
| 36 | -2.2 | 1.0 | 2.1 | -0.7 | 2.5 | 5.1 | 2.2 | 5.2 |
| 38 | -2.7 | 1.2 | 2.7 | -0.9 | 3.3 | 6.8 | 2.9 | 7.1 |
| 40 | -3.2 | 1.6 | 3.1 | -1.3 | 4.7 | 8.7 | 4.2 | 9.0 |
| 42 | -2.9 | 1.2 | 2.8 | -1.0 | 6.3 | 11.2 | 5.6 | 11.5 |
| 44 | -5.5 | 2.4 | 5.2 | -2.1 | 6.3 | 15.9 | 5.6 | 16.5 |
| 46 | -11.3 | 6.4 | 10.6 | -5.9 | 6.6 | 19.8 | 5.8 | 20.7 |
| 48 | -18.0 | 10.1 | 16.9 | -9.2 | 7.6 | 19.4 | 6.7 | 20.3 |
| 50 | -21.9 | 11.2 | 20.6 | -10.0 | 8.4 | 15.7 | 7.4 | 16.2 |
| 52 | -23.6 | 10.5 | 22.1 | -9.2 | 8.5 | 11.1 | 7.6 | 11.5 |
| 54 | -23.3 | 9.0 | 21.9 | -7.9 | 8.5 | 7.5 | 7.7 | 7.7 |
| 56 | -21.8 | 7.4 | 20.5 | -6.4 | 8.9 | 5.0 | 8.1 | 5.2 |
| 58 | -19.6 | 5.8 | 18.4 | -4.9 | 9.6 | 3.6 | 8.8 | 3.8 |
| 60 | -17.0 | 4.3 | 16.0 | -3.7 | 9.9 | 2.9 | 9.2 | 3.1 |
| 62 | -14.2 | 3.2 | 13.3 | -2.7 | 9.6 | 2.6 | 8.9 | 2.8 |
| 64 | -11.4 | 2.4 | 10.8 | -1.9 | 8.5 | 2.5 | 7.9 | 2.6 |
| 66 | -8.8 | 1.8 | 8.3 | -1.4 | 7.0 | 2.3 | 6.5 | 2.4 |
| 68 | -6.5 | 1.3 | 6.1 | -1.1 | 5.3 | 2.0 | 4.9 | 2.1 |
| 70 | -4.6 | 1.0 | 4.4 | -0.8 | 3.9 | 1.8 | 3.6 | 1.9 |
| 72 | -3.2 | 0.7 | 3.0 | -0.6 | 2.7 | 1.6 | 2.5 | 1.6 |
| 74 | -2.2 | 0.6 | 2.1 | -0.5 | 1.9 | 1.5 | 1.8 | 1.5 |
| 76 | -1.6 | 0.5 | 1.5 | -0.5 | 1.4 | 1.4 | 1.3 | 1.4 |
| 78 | -1.2 | 0.6 | 1.2 | -0.5 | 1.1 | 1.4 | 1.0 | 1.4 |
| 80 | -1.3 | 0.8 | 1.2 | -0.8 | 0.9 | 1.5 | 0.8 | 1.5 |

Table 3. (continued)

6.3 Semi-diurnal Hough components

The results obtained for symmetric Hough components of heating $J^2_{2,2}$, $J^2_{2,4}$, $J^2_{2,6}$ are shown in Fig. 7. Semi-diurnal Hough functions for s = 2 have previously been presented graphically (Groves, 1975) but may differ in sign from those used here which are positive at the equator if equatorially symmetric or increase at the equator with latitude if equatorially asymmetric. As with diurnal components the imaginary parts of $J^2_{2,n}$ are relatively small (of order $10^{-3}$) and will therefore be neglected. July values are slightly less than January values due to the increase of the Sun-Earth distance: October values are not shown being nearly the same as April values. $J^2_{2,2}$ shows very little annual variation due possibly to the form of $\Theta^2_{2,2}$ which unlike that for other modes considered has the same sign at all latitudes. Fig. 7 shows that at many heights the present values of $J^2_{2,2}$ are considerably lower than those of Chapman and Lindzen (1970) and that they compare quite well with those of Butler and Small (1963). $J^2_{2,4}$, $J^2_{2,6}$ have April and October values greatly exceeding January and July values in the region of 45 km whereas in the mesosphere January and July values greatly exceed April and October values: such differences are intricately related to the form of the ozone distribution and that of the Hough functions.

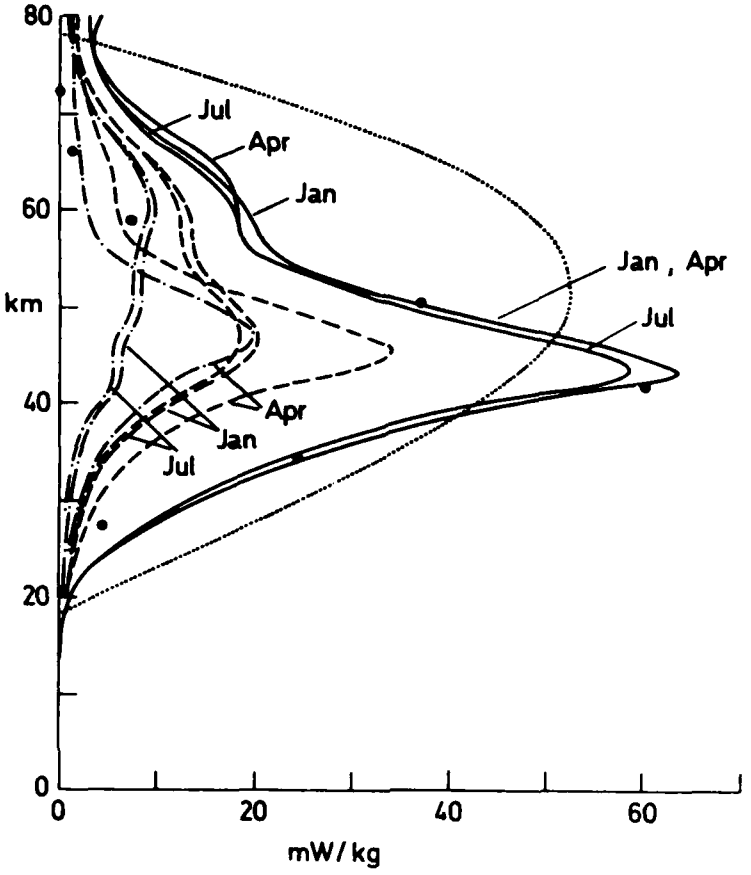


Fig. 7 Height profiles of Hough components of heating $J^2_{2,n}$ for n = 2,4,6. Key: ——— $J^2_{2,2}$; - - - - (-)$J^2_{2,4}$; —·—·—· $J^2_{2,6}$; ..... $J^2_{2,2}$ from Chapman and Lindzen (1970); • $J^2_{2,2}$ equinox values from Butler and Small (1963).

Fig. 8 shows the asymmetric components $J^2_{2,3}$, $J^2_{2,5}$ calculated for January and October; the July and April profiles differing only slightly from these with signs reversed. At the solstices, semi-diurnal heating is greater in the winter than the summer hemisphere as the shorter duration of daylight generates a larger Fourier component. This difference is further enhanced above 45 km by a large seasonal asymmetry in ozone densities (Table 1); and the rapid increase of heating rates with height apparent in Fig. 8 results. Semi-diurnal components are tabulated in Table 3.

## 7. Discussion

Formulae have been derived in §3 for the Hough components of ozone heating in the presence of a lower reflecting layer, account being taken in the theory of longitudinal dependences in the ozone distribution and the reflective properties of the underlying layer. A simple representation of surface and cloud reflectivities has been introduced (§ 5) which depends on longitude, but insufficient data are available for incorporating a longitudinal dependence into the ozone model introduced in § 4. Accordingly the Hough components presented here are those of migrating modes, i.e. those for which $s = m$, as these depend only on mean longitudinal

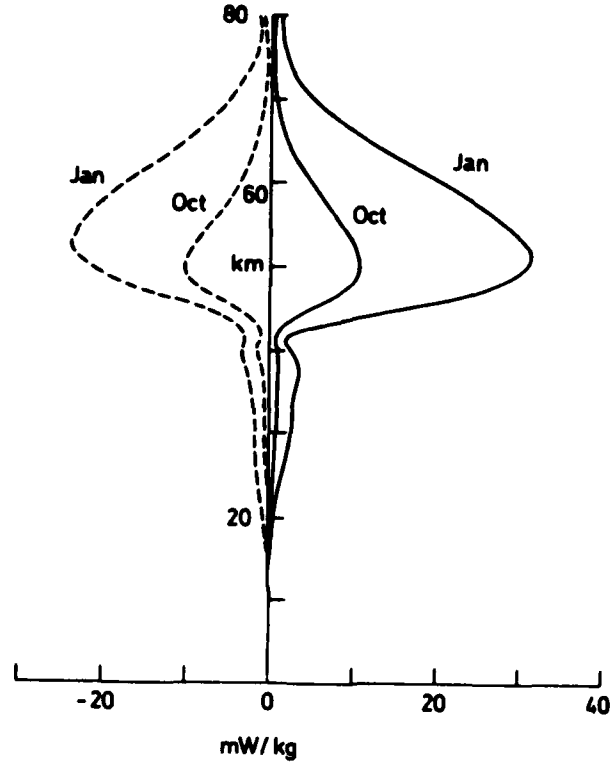


Fig. 8 Height profiles of Hough components of heating $J^2_{2,3}$, $J^2_{2,5}$. Key: ——— $J^2_{2,3}$; - - - - $J^2_{2,5}$.

properties.

Contributions from longitudinal variations in lower layer reflectivity, mainly in the cloud distribution, have been investigated as total cloudiness increases stratospheric heating by as much as 20 per cent at 30 km (§ 6.1); but the Hough components obtained for $s \neq m$ were mostly much less than 3 per cent of the corresponding $s = m$ components at the same height and have therefore not been presented. Furthermore such components maximize at about 32 km and would be significantly affected by any longitudinal ozone variations of the magnitude (12 per cent) previously indicated (§ 4).

A latitudinal and seasonal model of ozone densities (Table 1) has been adopted which is based on observational data in contrast to the 1964 photochemical model of Leovy which was used in earlier Hough component calculations. Although the available ozone data have obvious limitations, particularly at high latitudes and above 50 km, the model is expected to be a useful improvement on the 1964 theoretical model which has its own limitations, such as that of being based on pure oxygen reactions. For a hydrogen-oxygen-nitrogen system lower ozone concentrations are computed in the mesosphere due to hydrogen-oxygen reactions and also in the stratosphere due to nitrogen-oxygen reactions

(Shimazaki and Wuebbles, 1973; Park and London, 1974). In the lower stratosphere departures from radiational-photochemical equilibrium occur as ozone lifetimes increase sufficiently for vertical mixing to become an effective removal process, reducing concentrations still further.

Comparisons have been made in Figs. 4, 5 and 7 respectively between the newly calculated Hough components $J^1_{1,1}$, $J^1_{1,-2}$ and $J^2_{2,2}$ and those of earlier calculations (Lindzen, 1967; Chapman and Lindzen, 1970): the new values are considerably lower than the earlier values in height regions above and below the stratopause region of maximum heating in reasonable accord with the introduction of lower ozone densities.* The newly calculated $J^2_{2,2}$ have been compared in Fig. 7 with the evaluation of Butler and Small (1963) which was based on a simple ozone model devised from observational data: in view of the limited ozone and solar spectral UV data available at that time, the agreement between the two sets of results is better than expected.

In general the value of any Hough component depends intricately on the relation between the latitudinal profile of ozone and that of the particular Hough function. The decrease in April ozone densities towards low latitudes between 40 and 50 km (Table 1) would appear to be responsible for the minimum at 48 km in the components in Fig. 4; and

---

* Since this paper was finalized, reference has been obtained to Forbes, J.M. and Garrett, H.B. (1978) Geophys. Res. Lett. 5, 1013-1016 reporting similar significant differences from the heating profiles given by Chapman and Lindzen (1970).

also for the higher April values of $J^2_{2,4}$, $J^2_{2,6}$ in Fig. 5, the effect being in the cpposite sense due to the different form of the Hough functions in the two cases.

With regard to asymmetric Hough components a large part of the solstitial asymmetry in the mesosphere (Figs. 6 and 8) is generated by the asymmetry in mesospheric ozone densities shown in Table 1 which has winter values greatly in excess of summer values, being in the opposite sense to that predicted by photochemical theory (Park and London, 1974). This disagreement between observation and theory has previously been reported by Watanabe and Tohmatsu (1976) on the evidence of a series of rocket-borne solar UV radiometer measurements conducted since 1965 at 31° 15'N, 130° 05'E; a maximum winter-summer ratio of 2.8 being obtained at 65 km which is comparable with that shown by Table 1. Observational data above 50 km are sparse with values at the same latitude sometimes differing by a factor of 2 or more and hence the results in this paper above 50 km are particularly open to review in the light of further data on ozone densities.

Acknowledgements - Sponsorship has been provided for this work by the Air Force Geophysics Laboratory (AFGL), United States Air Force under Grant No. AFOSR - 77 - 3224. The assistance of Mr. Jonathan D. Groves with data preparation and computer processing on the GEC 4082 machines (EUCLID) at University College London is very gratefully acknowledged.

REFERENCES

ANDERSON, G.P., BARTH, C.A., CAYLA, F. and LONDON, J. (1969) Ann. Geophys. 25, 341-345.

BUTLER, S.T. and SMALL, K.A. (1963) Proc. R. Soc. Lond. A274, 91-121.

CHAPMAN, S. and LINDZEN, R.S. (1970) Atmospheric tides: thermal and gravitational. Dordrecht, Holland, D. Reidel Publishing Co.

CIRA (1972) COSPAR International Reference Atmosphere 1972, Akademie-Verlag, Berlin.

CLAPP, P.F. (1964) Mon. Wea. Rev. 92, 495-507.

COESA (1967) U.S. Standard Atmosphere Supplements, 1966, U.S. Government Printing Office, Washington, D.C.

DUETSCH, H.U. (1974) Can. J. Chem. 52, 1491-1504.

FREDERICK, J.E., GUENTHER, B.W. and HEATH, D.F. (1977) Beitr. Phys. Atmos. 50, 496-507.

GHAZI, A., EBEL, A. and HEATH, D.F. (1976) J. Geophys. Res. 81, 5365-5373.

GROVES, G.V. (1975) J. Brit. Interplan. Soc. 28, 797-809.

GROVES, G.V. (1979) Notes on obtaining the eigenvalues of Laplace's tidal equation, in Interim Scientific Report No. 3, AFOSR-77-3224, Department of Physics and Astronomy, University College London, Gower Street, London WC1E 6BT, England, 31 December 1979.

HILSENRATH, E., HEATH, D.F. and SCHLESINGER, B.M. (1979) J. Geophys. Res. 84, 6969-6979.

HONG, S-S. and LINDZEN, R.S. (1976) J. Atmos. Sci. 33, 135-153.

KATAYAMA, A. (1966) J. Meteor. Soc. Japan 44, 381-401.

KATAYAMA, A. (1967) J. Meteor. Soc. Japan 45, 1-25.

KHRUGIAN, A. Kh. (1973) The physics of atmospheric ozone, Gidrometeoizdat, Leningrad. Published in English translation by IPST-Keter and distributed by John Wiley and Sons, Ltd., 1975.

KRUEGER, A.J. (1973) Pure and App. Geophys. 106-108, 1272-1280.

KRUEGER, A.J., GUENTHER, B., FLEIG, A.J., HEATH, D.F., HILSENRATH, E., McPETERS, R. and PRABHAKARA, C. (1980) Phil. Trans. R. Soc. Lond. A296, 191-204.

KRUEGER, A. J., HEATH, D.F. and MATEER, C.L. (1973) Pure and App. Geophys. 106-108, 1254-1263.

KRUEGER, A.J. and MINZNER, R.A. (1976) J. Geophys. Res. 81, 4477-4481.

LACIS, A.A. and HANSEN, J.E. (1974) J. Atmos. Sci. 31, 118-133.

LEOVY, C. (1964) J. Atmos. Sci. 21, 238-248.

LINDZEN, R.S. (1967) Quart. J. R. Met. Soc. 93, 18-42.

LINDZEN, R.S. and HONG, S-S. (1974) J. Atmos. Sci. 31, 1421-1446.

LIOU, K-N., FREEMAN, K.P. and SASAMORI, T. (1978) Tellus 30, 62-70.

LONDON, J. (1963) Beitr. Phys. Atmos. 36, 254.

LONDON, J., FREDERICK, J.E. and ANDERSON, G.P. (1977) J. Geophys. Res. 82, 2543-2556.

LUCAS, R.J. (1978) A latitudinal and seasonal ozone model to 75 km, in Scientific Report AFOSR-77-3224 by Groves, G.V. and Lucas, R.J., Department of Physics and Astronomy, University College London, Gower Street, London WC1E 6BT, England, 31 December 1978.

PARK, J.H. and LONDON, J. (1974) J. Atmos. Sci. 31, 1898-1916.

PRABHAKARA, C., RODGERS E.B., CONRATH, B.J., HANEL, R.A. and KUNDE, V.G. (1976) J. Geophys. Res. 81, 6391-6399.

RAMANATHAN, K.R. and KULKARNI, R.N. (1960) Quart. J. R. Met. Soc. 86, 144-155.

SHAW, Napier (1942) Manual of Meteorology, Vol. II, Comparative Meteorology, Cambridge University Press.

SHIMAZAKI, T. and WUEBBLES, D.J. (1973) Pure and App. Geophys. 106-108, 1446-1463.

THEKAEKARA, M.P. (1973) Solar Energy 14, 109-127.

WATANABE, T. and TOHMATSU, T. (1976) Rep. Ionosphere and Space Res. Japan 30, 47-50.

WILCOX, R.W., NASTROM, G.D. and BELMONT, A.D. (1977) J. Appl. Meteor. 16, 290-298.

YAMAMOTO, G., TANAKA, M. and OHTA, S. (1974) J. Meteor. Soc. Japan 52, 61-68.